Mágneses alakemlékező ötvözetek
vagy
óriás magnetostrikciót mutató anyagok

Varga Lajos Károly

MTA, Wigner F.K., Sz.F.I.

What is SMART material?

Material that changes the coefficient of one

SHAPE

of its properties in response to an external

H field SHAPE

stimulus and when this change can be used

H field

to control the stimulus.

Active Materials-Definition-coupling

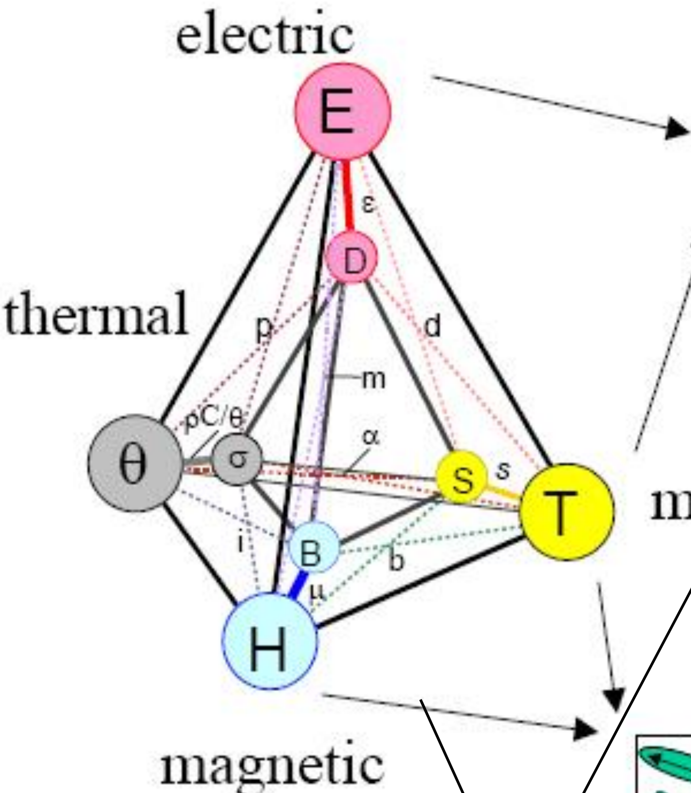

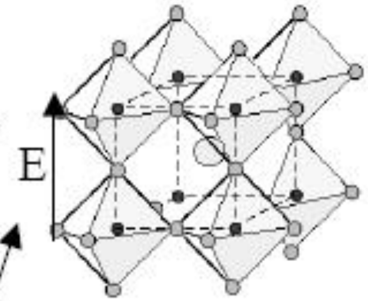

Piezoelectric
Curie in 1880

Pb-Mg-Nb

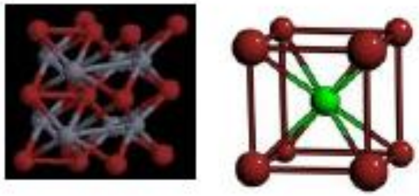

Shape Memory
Chang & Read
1932

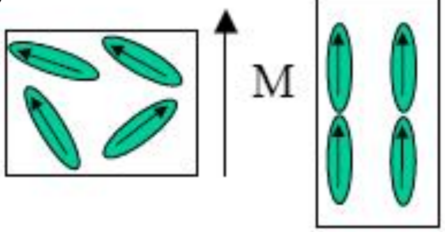

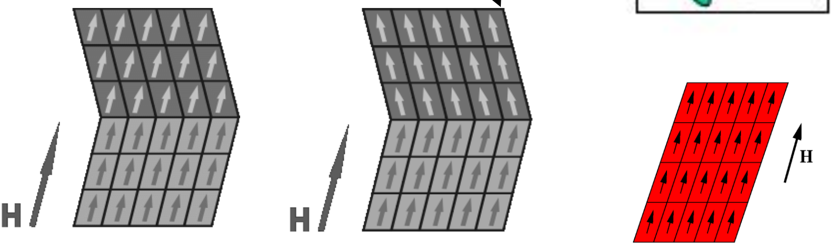

Magnetostrictive
Joule 1842

Tb-Fe-Dy

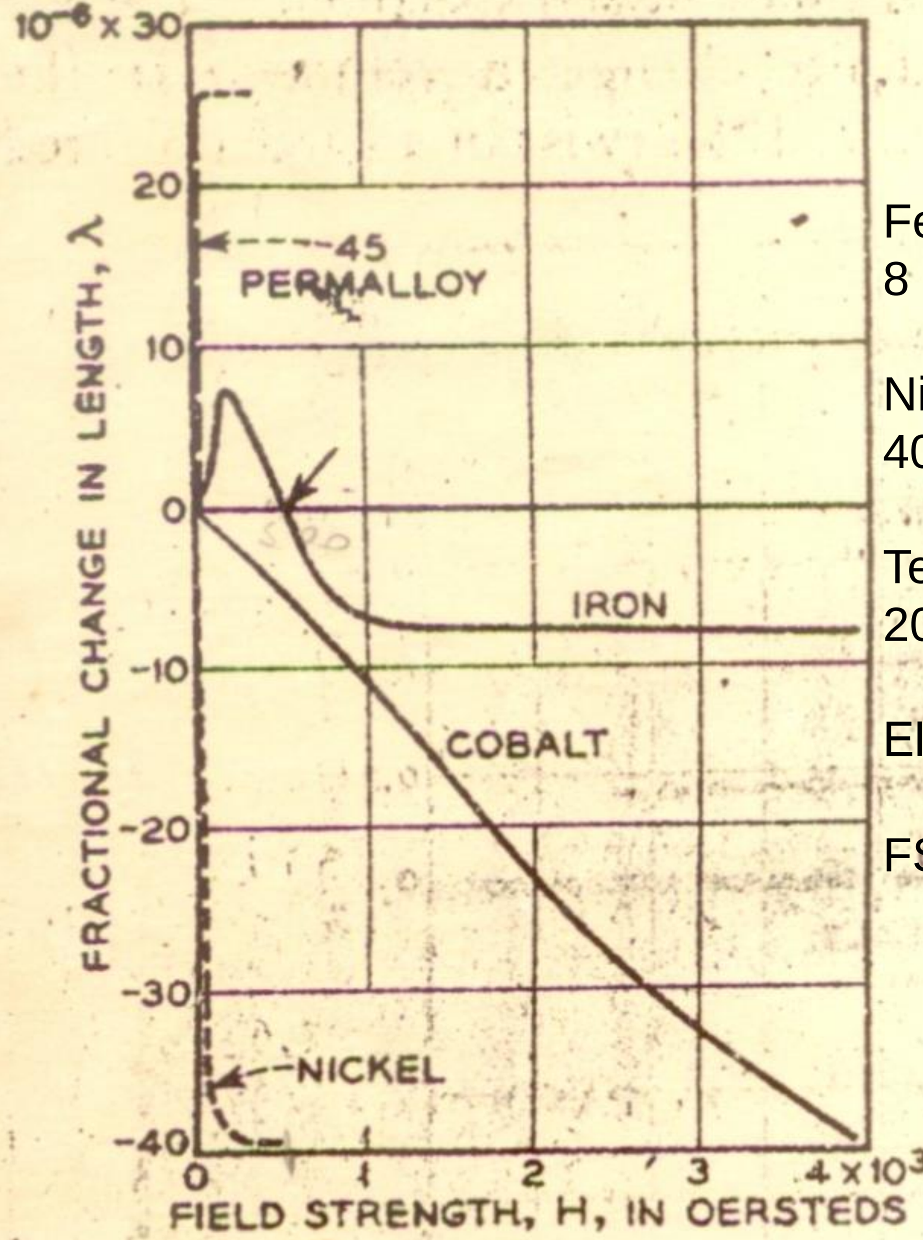

Fig. 13–48. Magnetostriction at high field strengths.

Fe
8 ppm = 8x10-4 %

Ni
40 ppm = 4x10-3 %

Terfenol
2000 ppm =0.2 %

Elasztikus határ 0.1-0.2 %

FSMA : 10 %

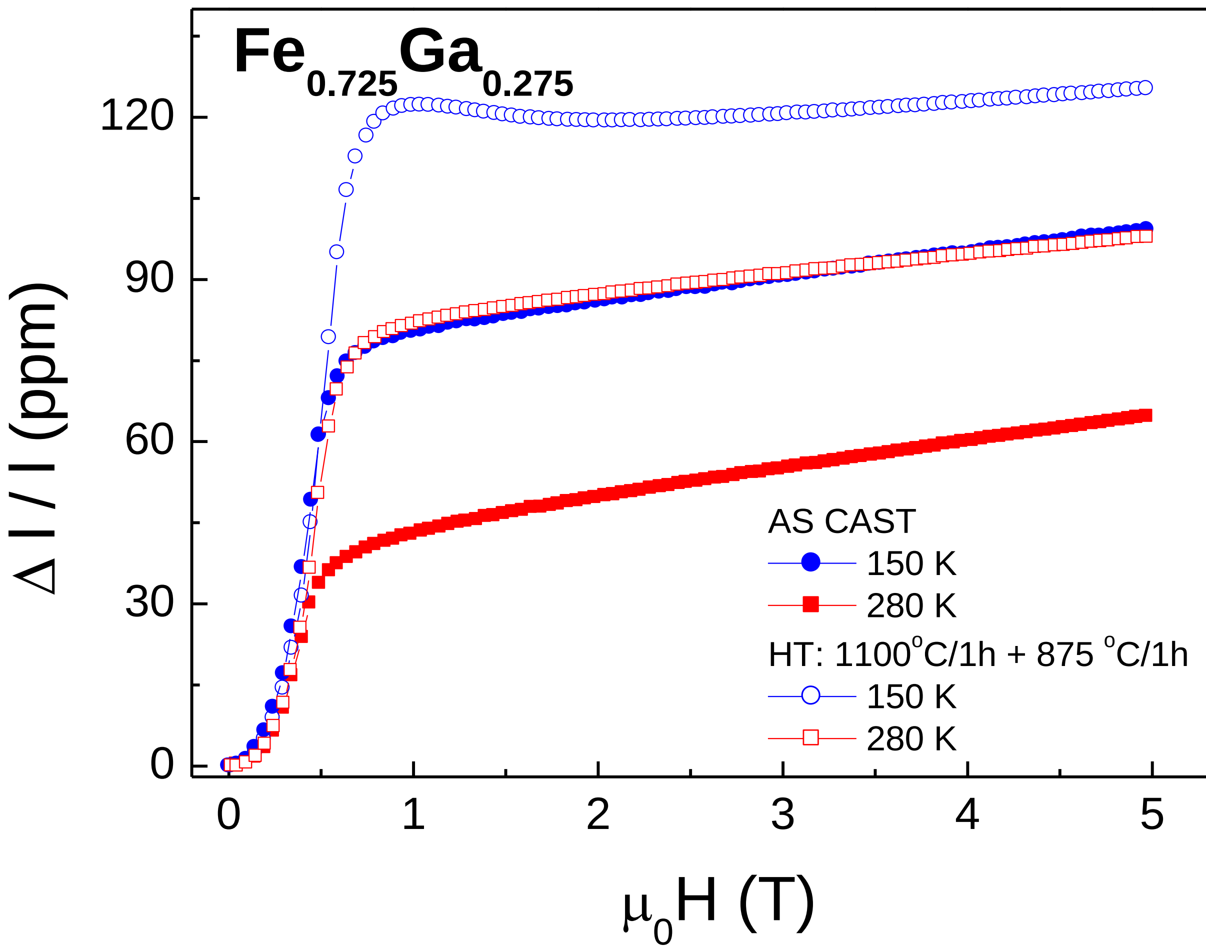

$Fe_{0.725}Ga_{0.275}$
$\Delta l / l$ (ppm)
$\mu_0 H$ (T)
0
30
60
90
120
0
1
2
3
4
5
AS CAST
150 K
280 K
HT: 1100°C/1h + 875 °C/1h
150 K
280 K

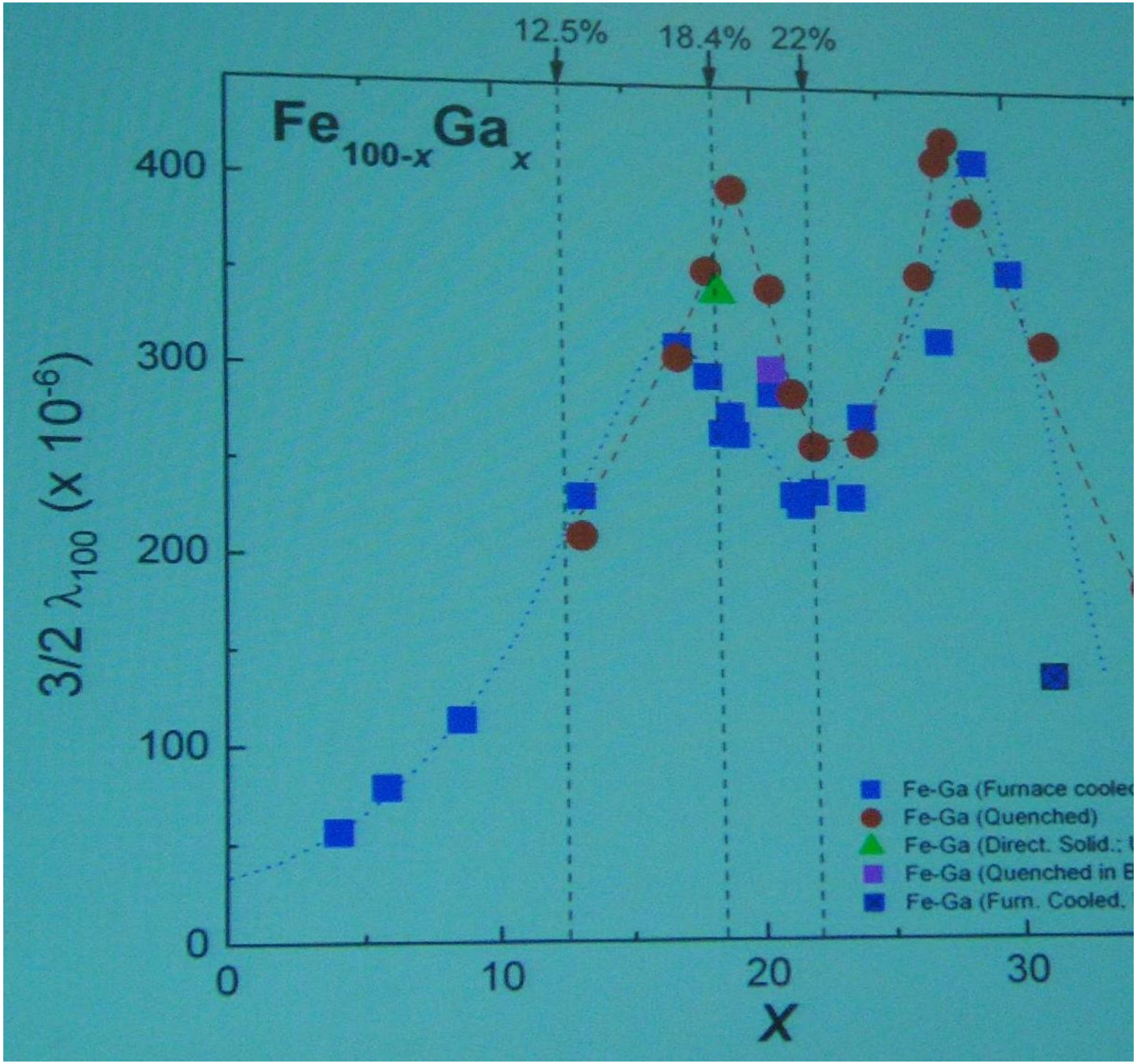

12.5%
18.4%
22%
$Fe_{100-x}Ga_x$
400
300
200
100
0
10
20
30
$3/2\ \lambda_{100}\ (\times 10^{-6})$
x
Fe-Ga (Furnace coole
Fe-Ga (Quenched)
Fe-Ga (Direct. Solid.;
Fe-Ga (Quenched in B
Fe-Ga (Furn. Cooled,

	Piezoelect. (PZT)	Magnetostr. (Terf.-D)	SMA (NiTi)	MSMA (Ni-Mn-Ga)
Control mode	electric	magnetic	heat	magnetic
Max. strain (%)	0.1-0.6	0.15-0.2	2-8	6-10
Blocking stress (MPa)	100	70	250	3
Response time	μs	ms	s	ms

Összehasonlító táblázata a különböző aktív anyagoknak

Revolution of Electromechanics

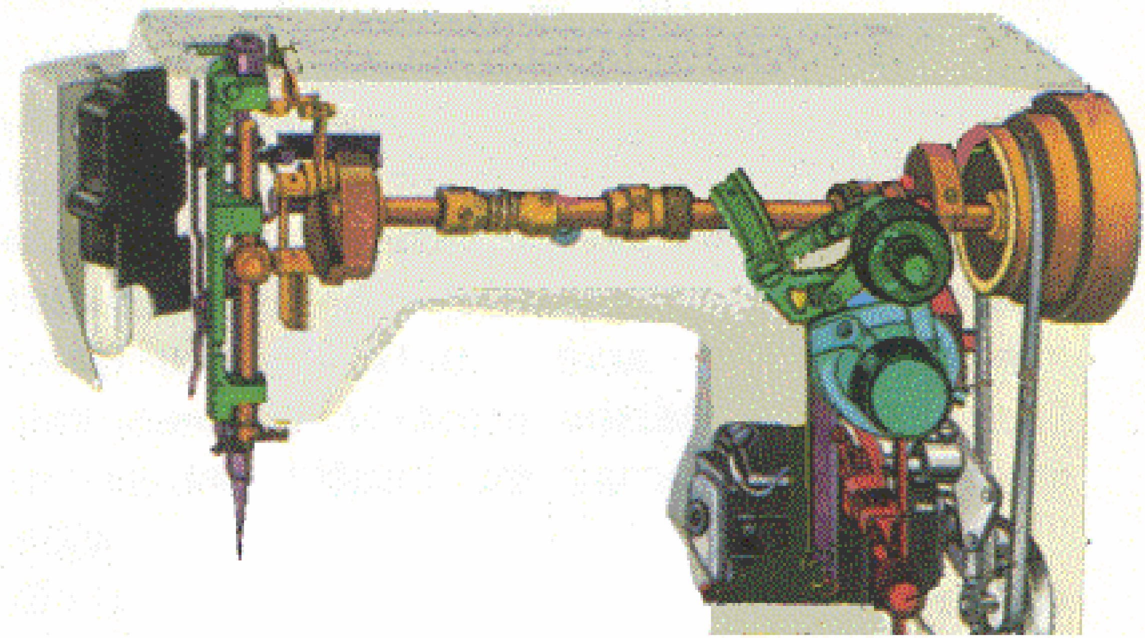

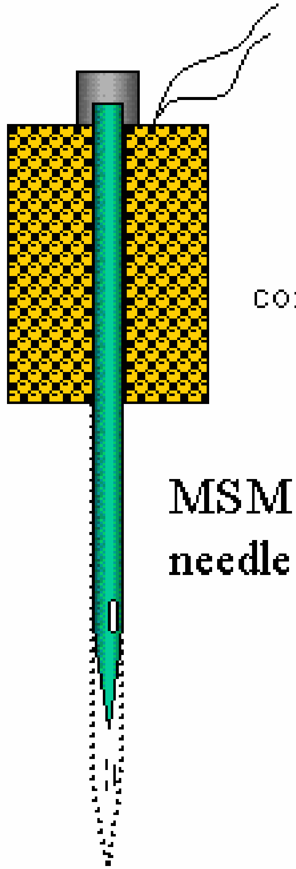

Magnetically controlled shape memory materials (MSM)
replace machines

AdaptaMat

A basic actuator structure

A basic actuator consists of a coil
and a MSM element.

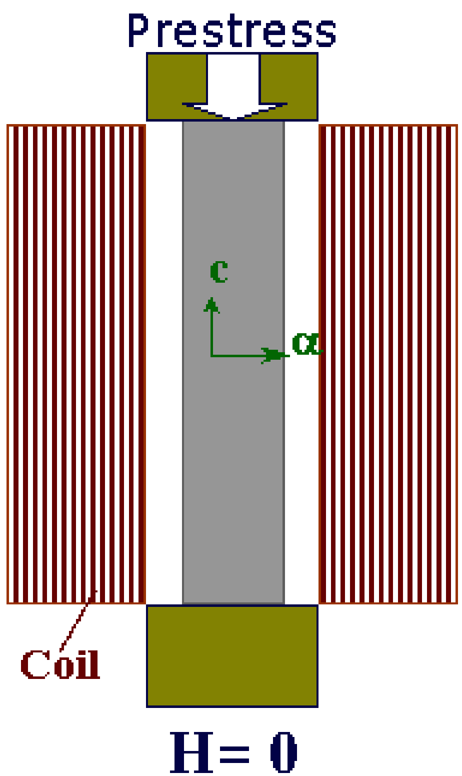

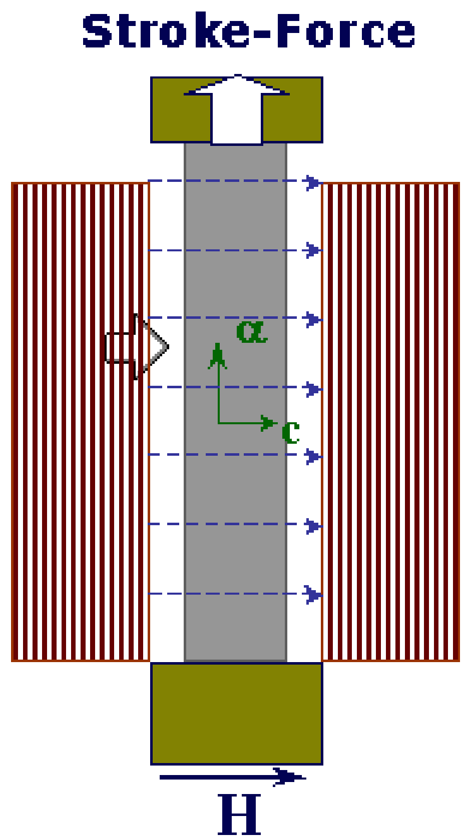

Actuator

An actuator produced by AdaptaMat which controls pressure in a pneumatic valve.

When magnetic field is applied, the MSM element elongates in the direction perpendicular to the magnetic field.

MAGNETICALLY CONTROLLED ACTUATORS BASED ON Ni-Mn-Ga (ADAPTAMAT)

A5-2

A06-3

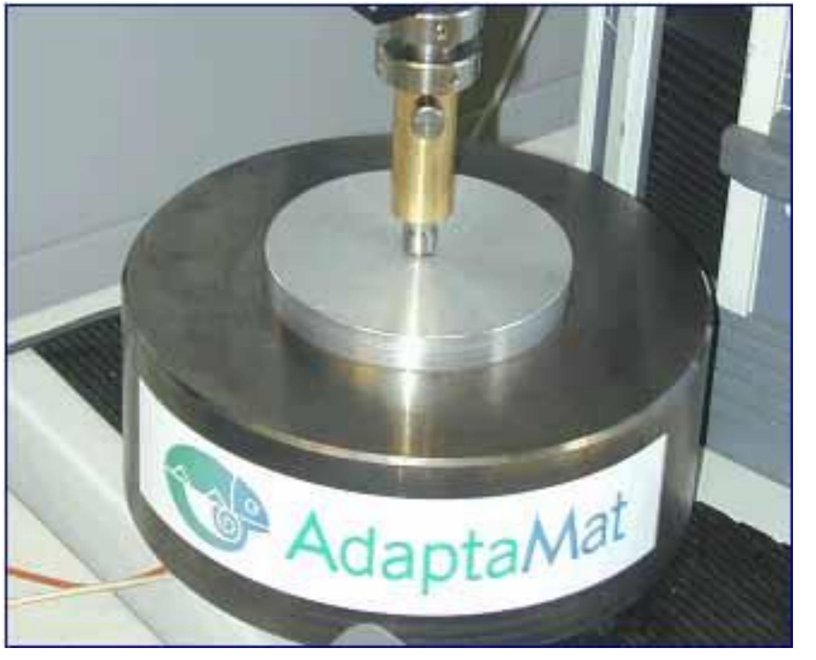

A1-2000

Displacement 0,6 – 5 mm,

Force – up to 1000 Newtons,

Frequency 300 – 1000 Hz

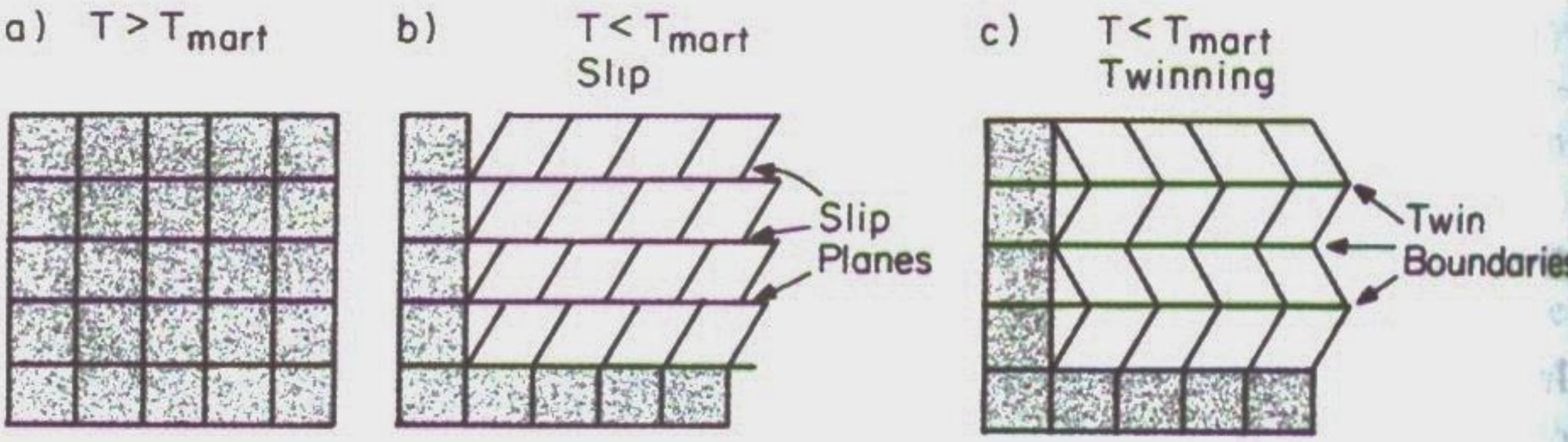

Figure 7A1 Schematic representation of an austenitic material (*a*) On cooling to $T < T_{\mathrm{mart}}$, the transformation strain associated with the appearance of the low-temperature phase can be accommodated by either slip (*b*) or twinning (*c*).

Strain can be reduced by introducing twins

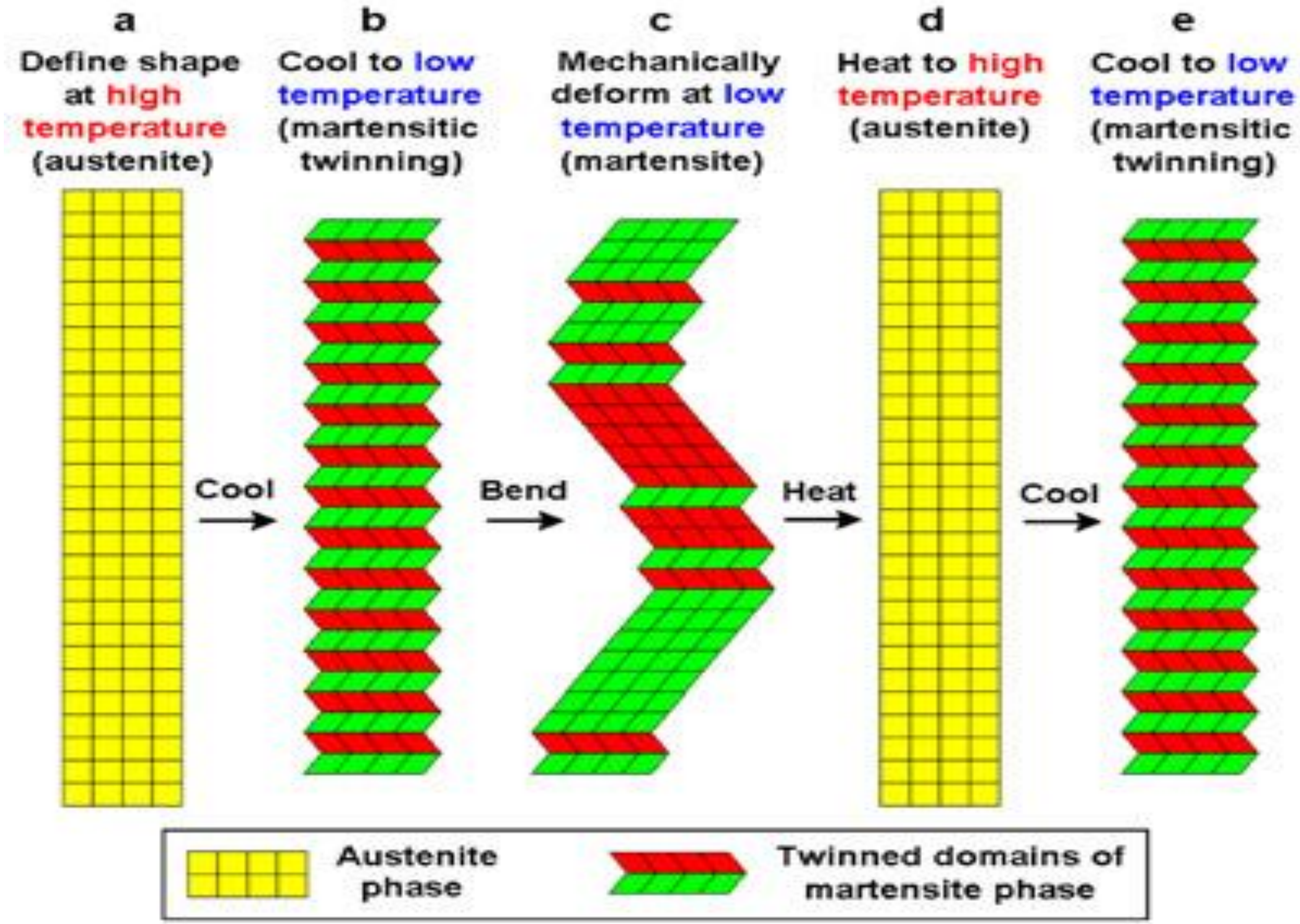

- Deformation may take different direction in different regions of the sample.
- These structural domains have well defined boundaries (twin boundary) and are called variants.

no magic, no will power

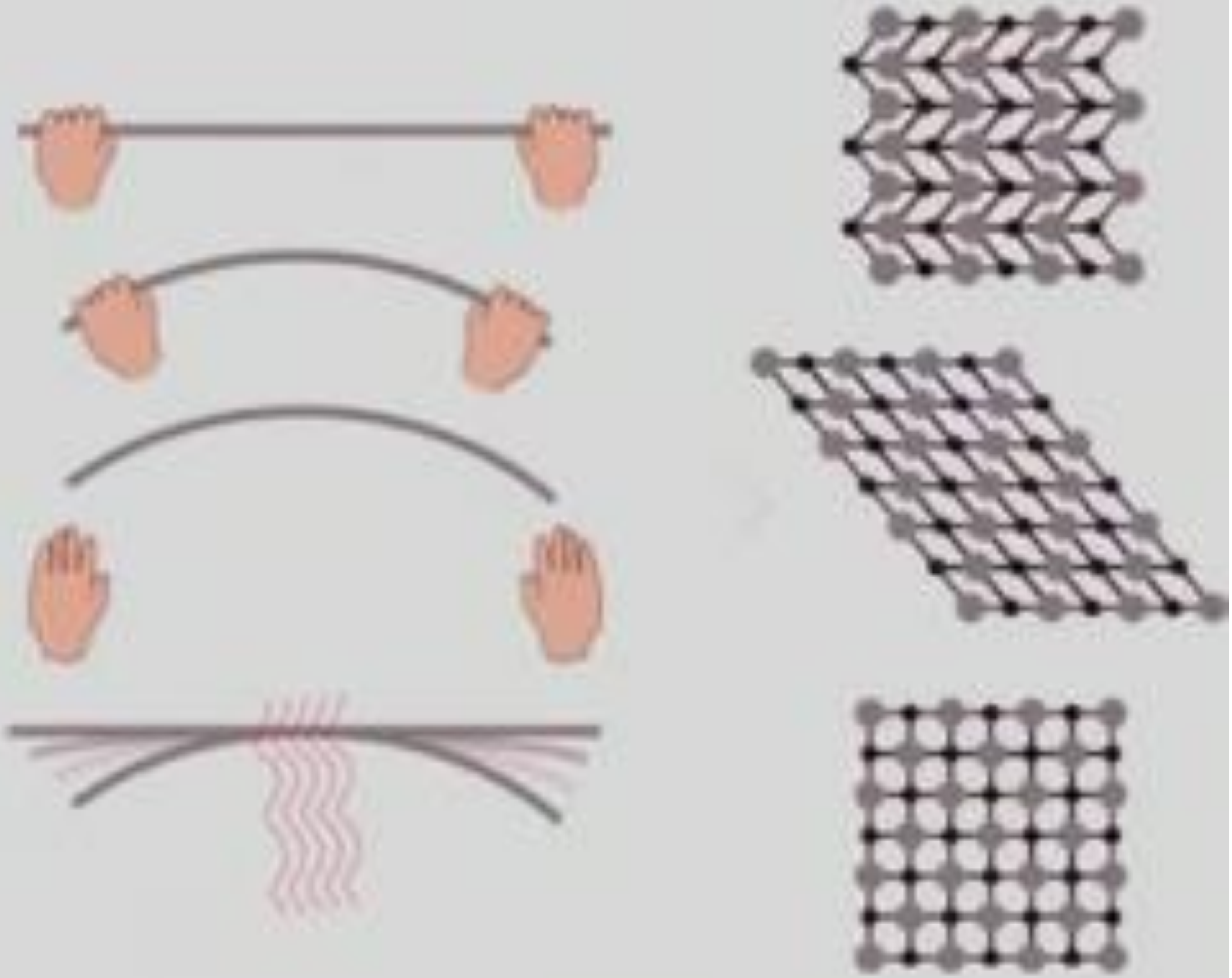

Shape Memory Alloy

- A material, previously deformed in MARTENSITE (the low temperature) phase-recovers its original shape, when heated up to the austenite-the high temperature phase.

- The martensitic transformation occurs across a given range of temperature (M_s to M_f, from austenite to martensite and A_s to A_f, from martensite to austenite)

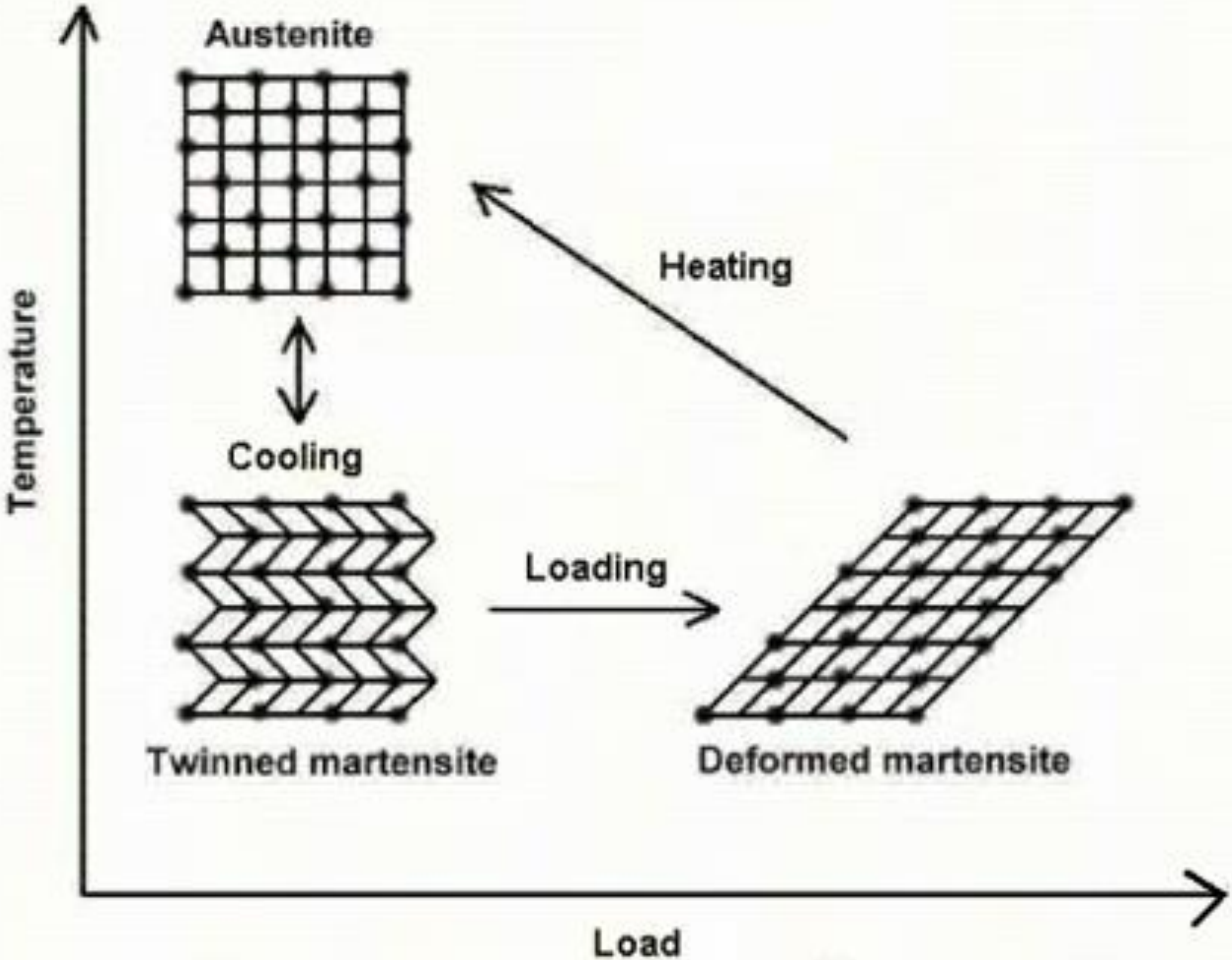
Austenite
Heating
Temperature
Cooling
Loading
Twinned martensite
Deformed martensite
Load

Deformation Characteristics

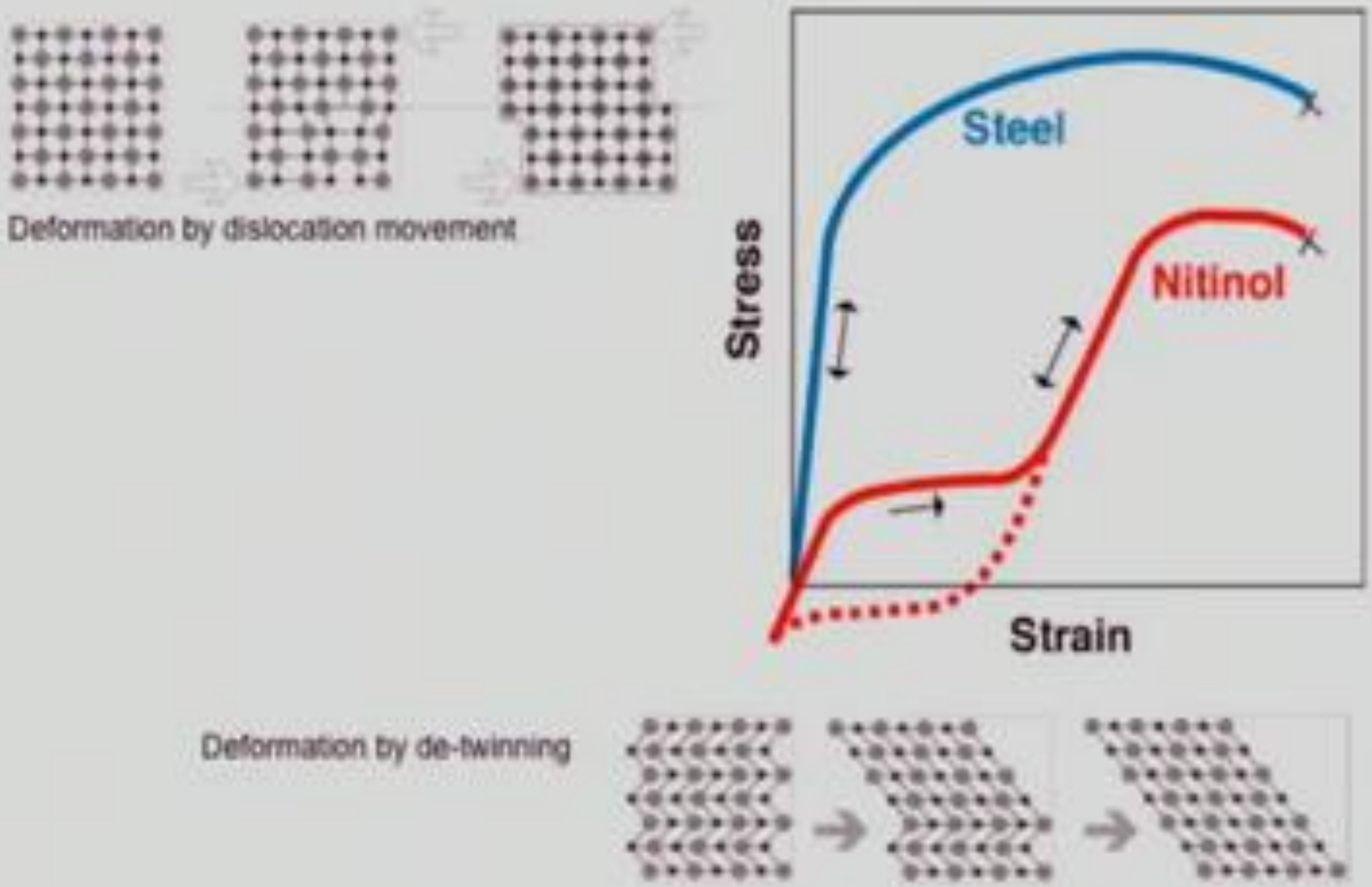

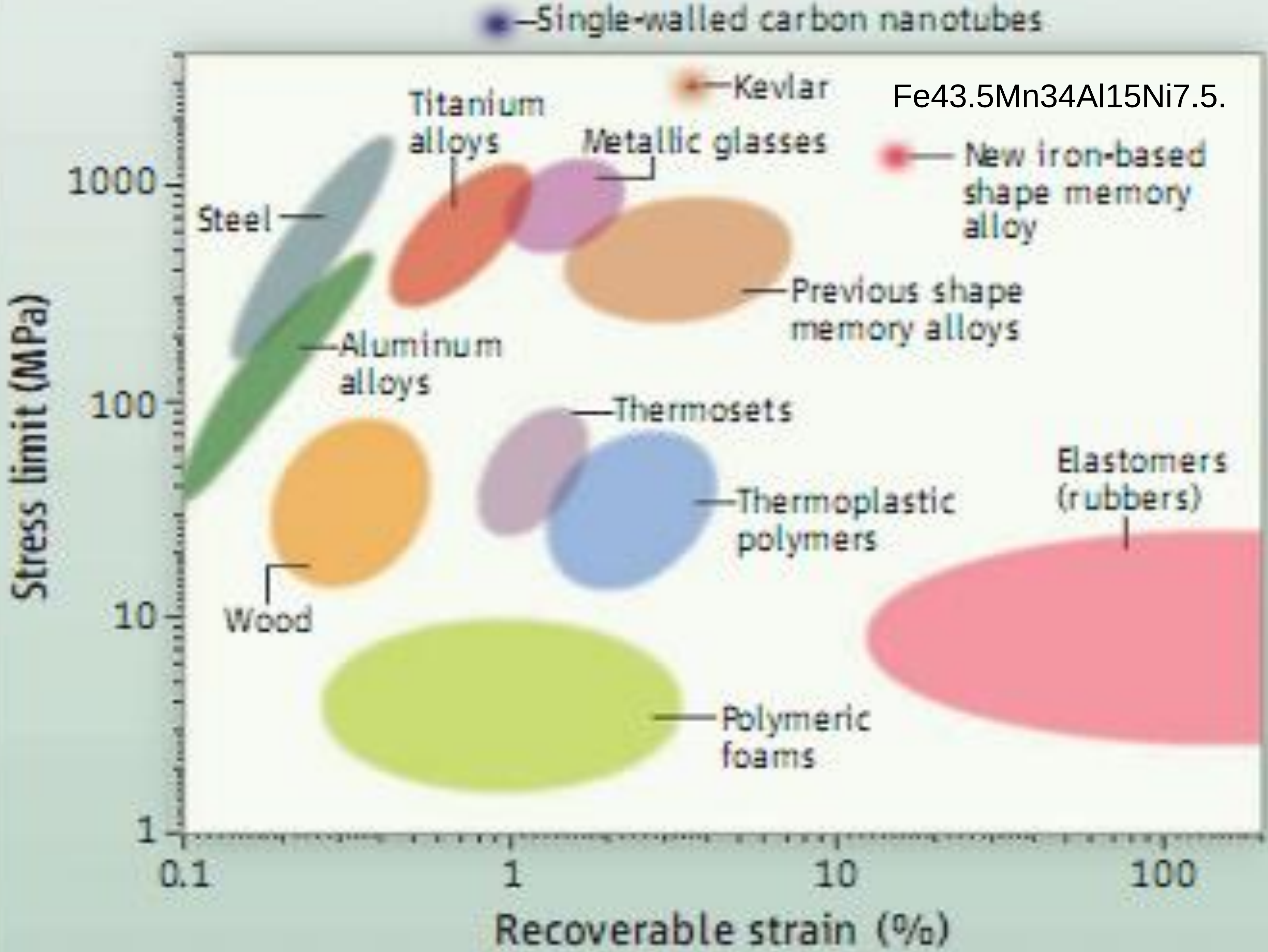
Single-walled carbon nanotubes
Kevlar
Fe43.5Mn34Al15Ni7.5.
Titanium alloys
Metallic glasses
New iron-based shape memory alloy
Steel
Previous shape memory alloys
Aluminum alloys
Thermosets
Elastomers (rubbers)
Thermoplastic polymers
Wood
Polymeric foams
Stress limit (MPa)
1000
100
10
1
0.1
1
10
100
Recoverable strain (%)

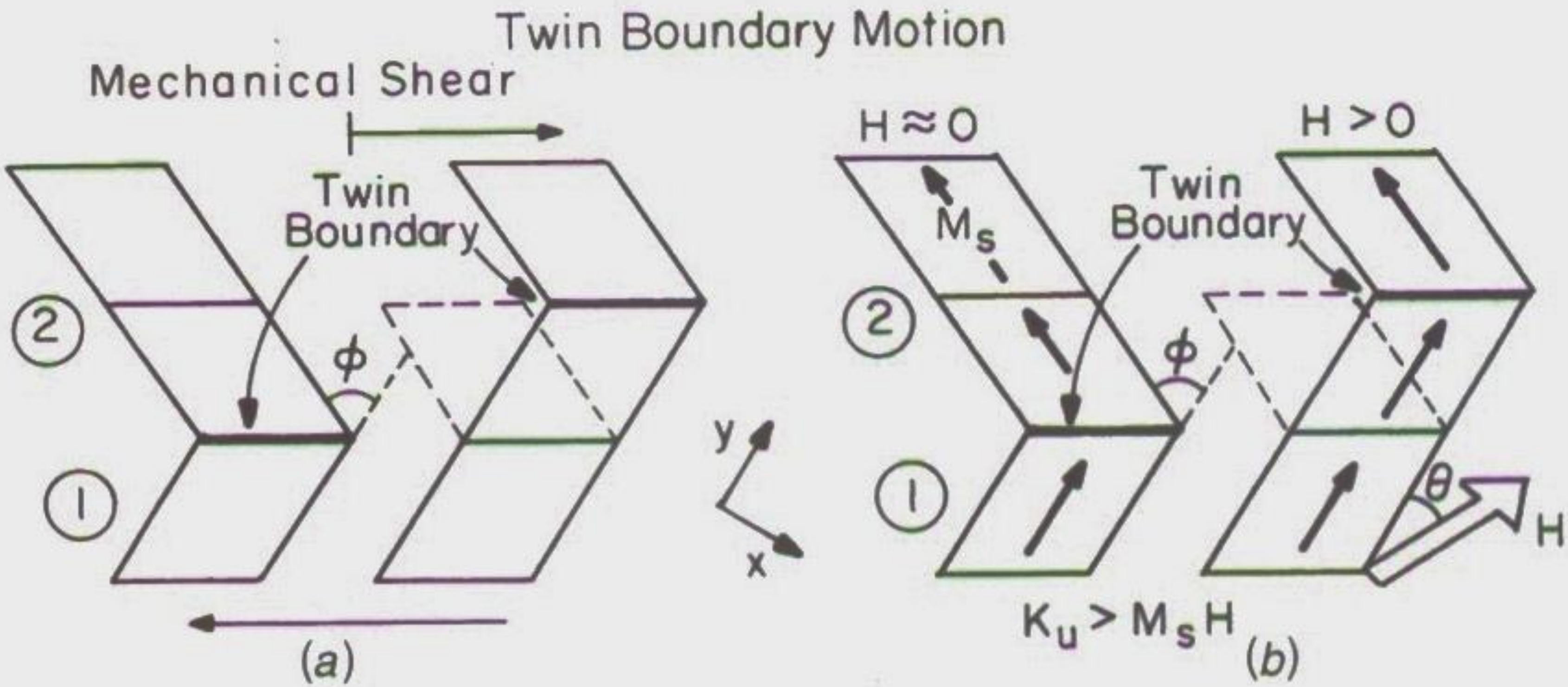

Figure 7A.2 A twinned, martensitic material can respond to a shear stress by twin boundary motion, leading to what appear to be large plastic deformations (*a*). If the martensitic phase is magnetic with a strong magnetocrystalline anisotropy that changes direction across the twin boundary, application of a magnetic field generates a Zeeman pressure on the twin boundary (*b*). This pressure tends to grow variant 1 at the expense of variant 2.

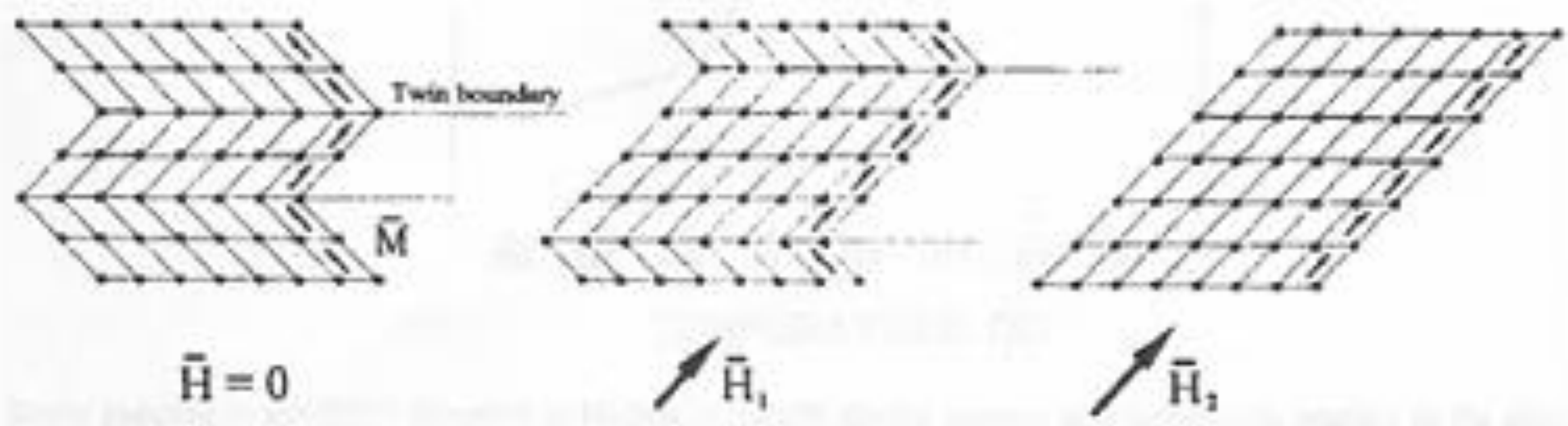

Figure 1: Schematic drawing of the ferromagnetic shape memory effect[5]

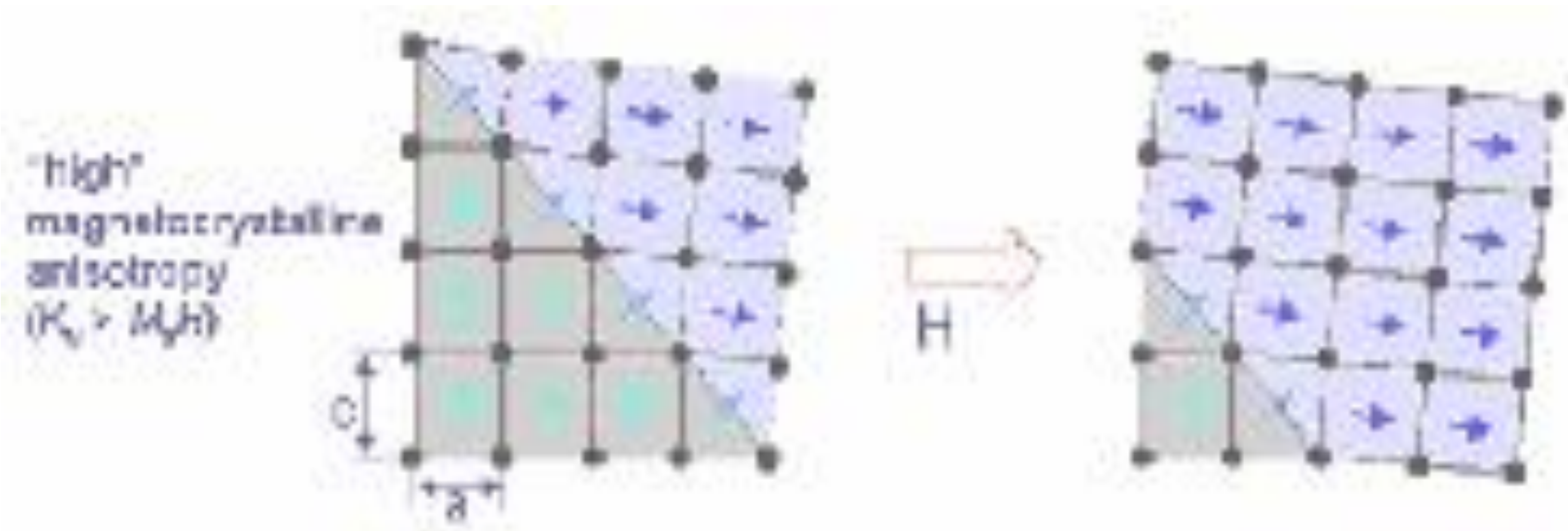

Magnetic Shape Memory Effect

Ferromagnetic shape memory alloys (FSMA) are smart materials possessing not only ferromagnetic as well as thermal shape memory properties but also large magnetic field induced strains. In single crystalline Ni_2MnGa bulk material, strains as large as 10% have been realized.

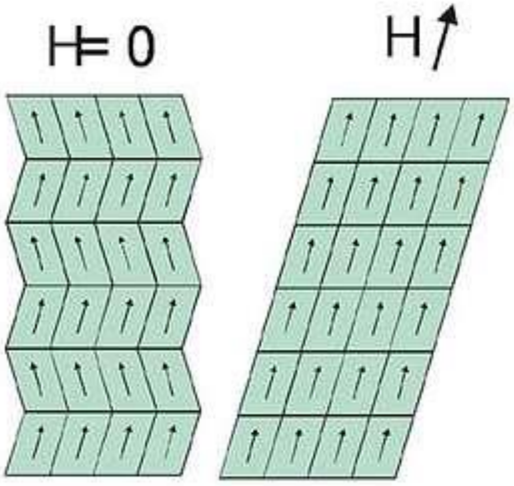

Principle of magnetic field induced re-orientation of martensitic variants.

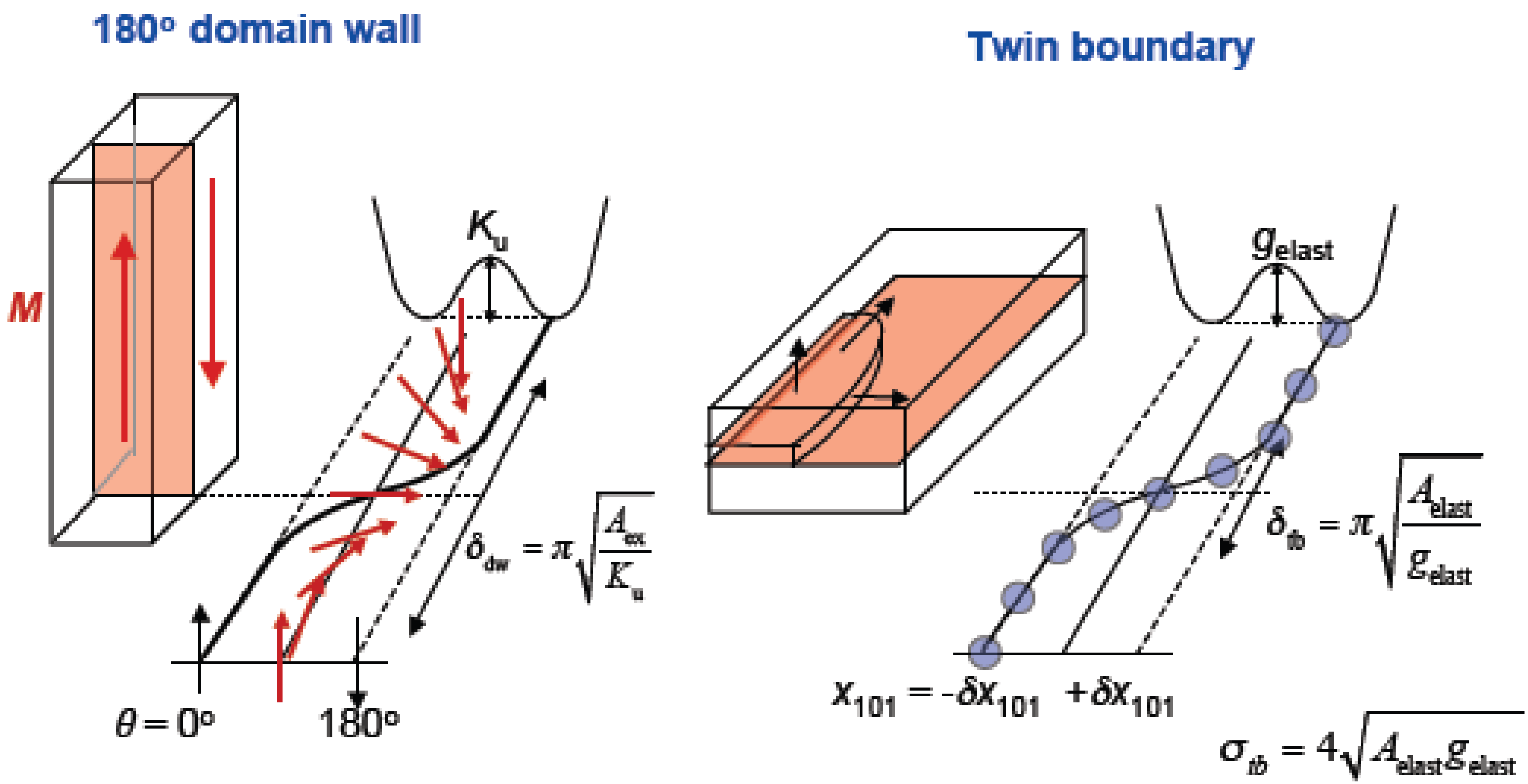

$\theta(vt\text{-}x_0)$ or δx_{101} unchanged with position, x_0

Energy density, $\sigma_{dw} = 4\sqrt{AK_u}$, unchanged with position in absence of defects

Clapp:

*Critical nucleus has $\varepsilon < \varepsilon_0$ with diffuse interface

$$g = \int \left[g(\varepsilon) + k(\nabla \varepsilon)^2 \right] dV$$

Strain energy — diffuse interface

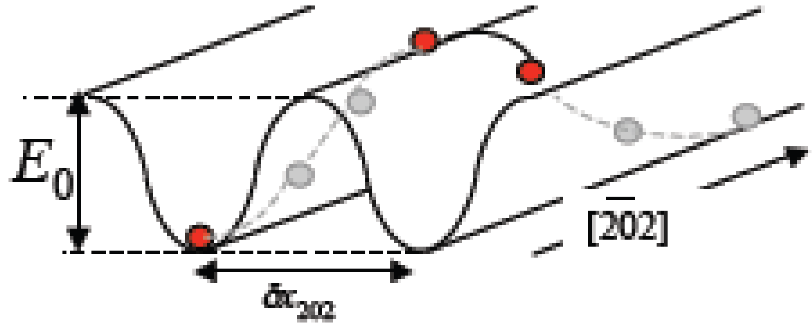

Twin dislocation energy
$G \approx 15$ meV/atom

Magnetic domain wall:

$$g_{\rm mag} = \int \left[g(\theta) + A(\nabla \theta)^2 \right] dV$$

Anisotropy energy — Exchange energy

Minimizing these integrals gives interface energy density, σ, and interface thickness , δ

$$g_2 = -M_s H \cos\theta_2 + K_u \cos^2\theta_2$$

$$g_1 = -M_s H$$

$$g = f_1 g_1 + (1 - f_1) g_2$$

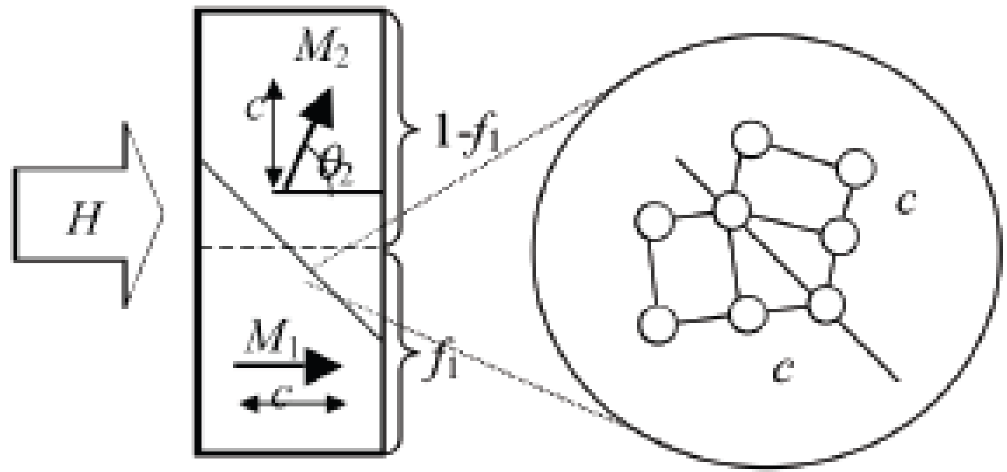

Minimize *g* with respect to θ and δf ; use $h = H/H_a$

$$\delta f = \frac{2K_u h(1 - h/2) - \sigma\varepsilon_0}{2C\varepsilon_0^2}$$

$$\delta f = \frac{2K_u h(1 - h/2) - \sigma\varepsilon_0}{2C\varepsilon_0^2}$$

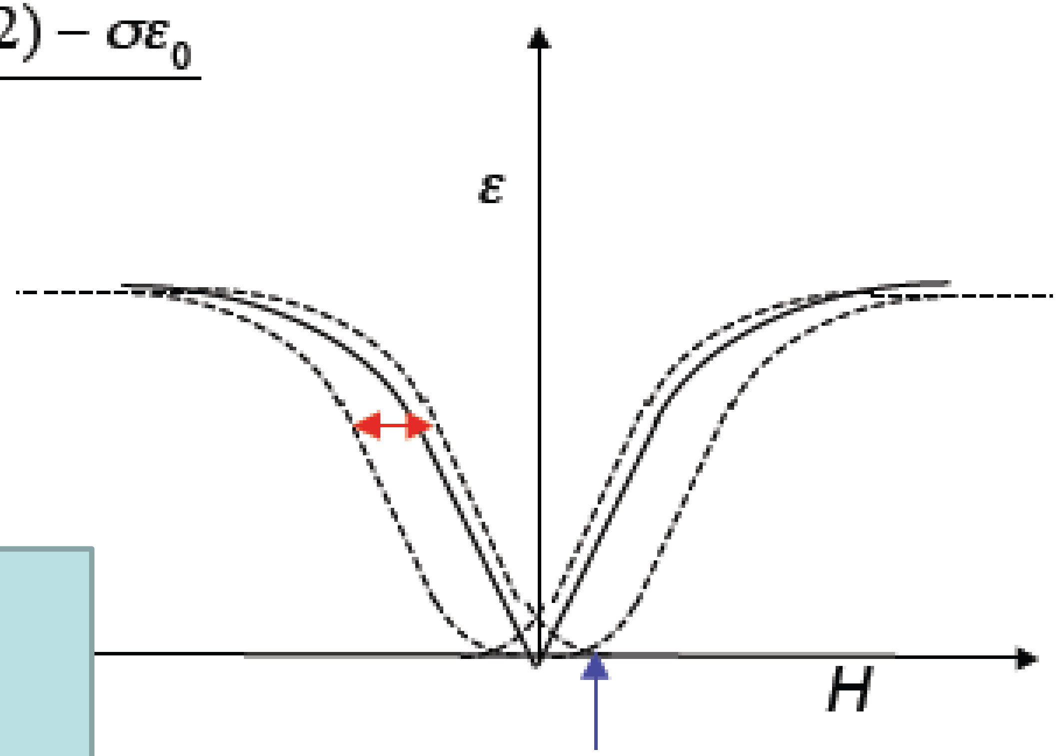

Requirements for FSM Effect

- The material should be ferromagnetic and exhibit martensitic transformation, thus $T_{M \rightarrow A} < T_C$
- The magnetic anisotropy energy should be greater than the energy needed to move the twin boundary.
- Till now, numerous FSMA systems have been investigated e.g.

  Ni-Co-Al, Co-Nb-Sn, Ni-Mn-Ge and Ni_2MnAl

Magnetic domains and twin bands

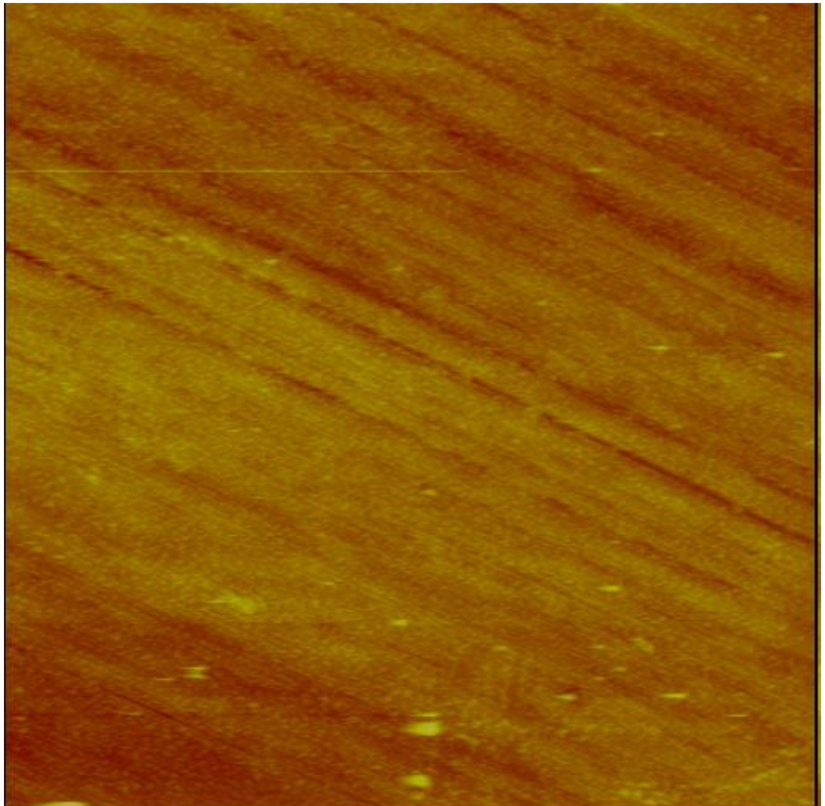

Topography image

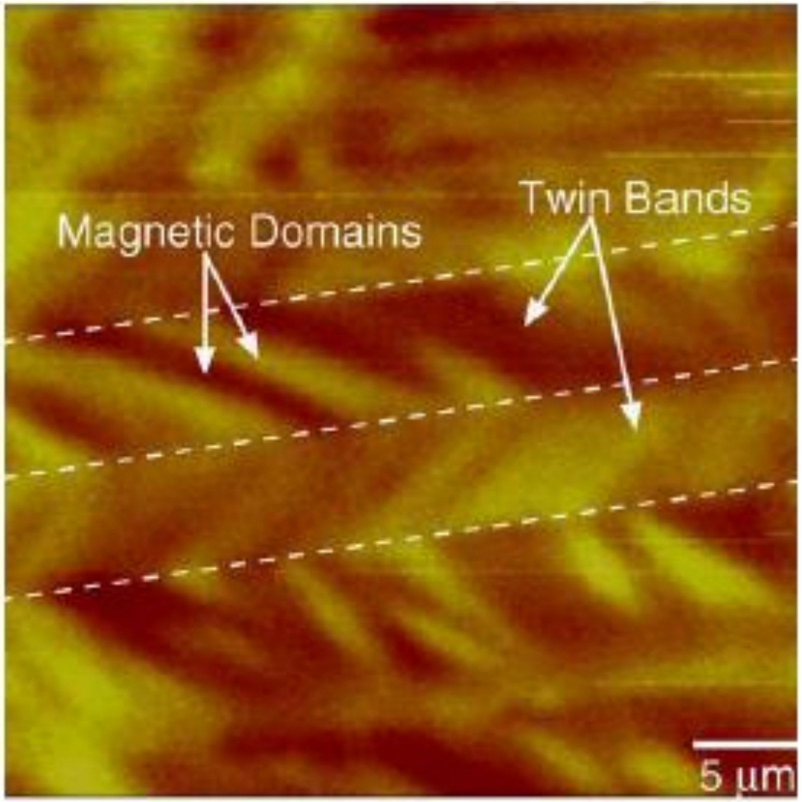

MFM image

Magnetic force microscopy image of $Ni_{2.23}Mn_{0.8}Ga$ in the martensitic phase at room temperature clearly shows the twin bands (width 10 micron) and magnetic domains (width 2-3 microns)

C. Biswas, S. Banik, A. K. Shukla, R. S. Dhaka, V. Ganesan, and S. R. Barman, , Surface Science, 600, 3749 (2006).

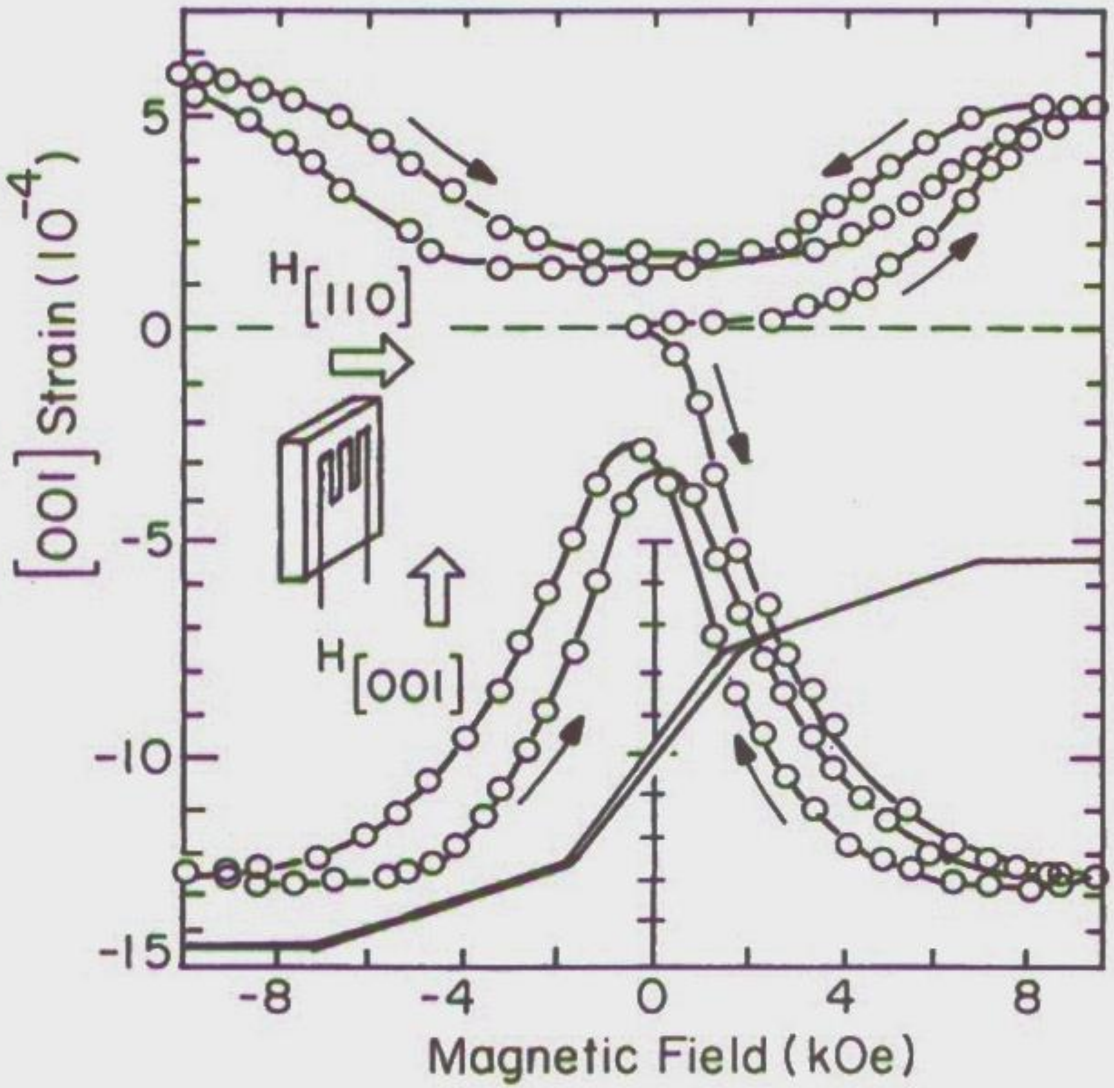

Figure 7A.3 Strain measured along [001] in a single crystal of Ni_2MnGa in fields directed parallel and perpendicular to the strain gauge. $T = -8°C$. Note that the sample contracts in a field parallel to the gauge. The same experiment done above the transformation temperature produced strains with similar field dependence but one-tenth the magnitude. [After Ullakko et al. (1996)].

Progress in FSMA

- The work on FSMA started in 1996 when both ferromagnetism and shape memory effect were observed in Ni-Mn-Ga alloy by K.Ullako in R.C. O'Handley's group .

- In 1999, **0.3%** strain was reported by Wu et. al., **1.3%** by Tickle et al., **4 %** by James et al., **4.3 %** by Tickle et al.

- In 2000, **5 %** and **5.1%** reported by Heckzo et.al , **5.7 %** by Murray et. al.

- Later, Murray et al. reported **6.2%** strain and Srivastava et al. reached **5.9%** strain at composition around $Ni_{50}Mn_{28}Ga_{22}$ and $Ni_{49}Mn_{29}Ga_{22}$ respectively almost reaching the theoretical maximum.

- A .Sozinov et. al. obtained a maximum strain of **9.5%** in Ni50Mn30Ga20.

Till now this is the maximum strain obtained in related crystal. Since then lot of work has been done on this alloy.

Ni_2MnGa is a Heusler alloy

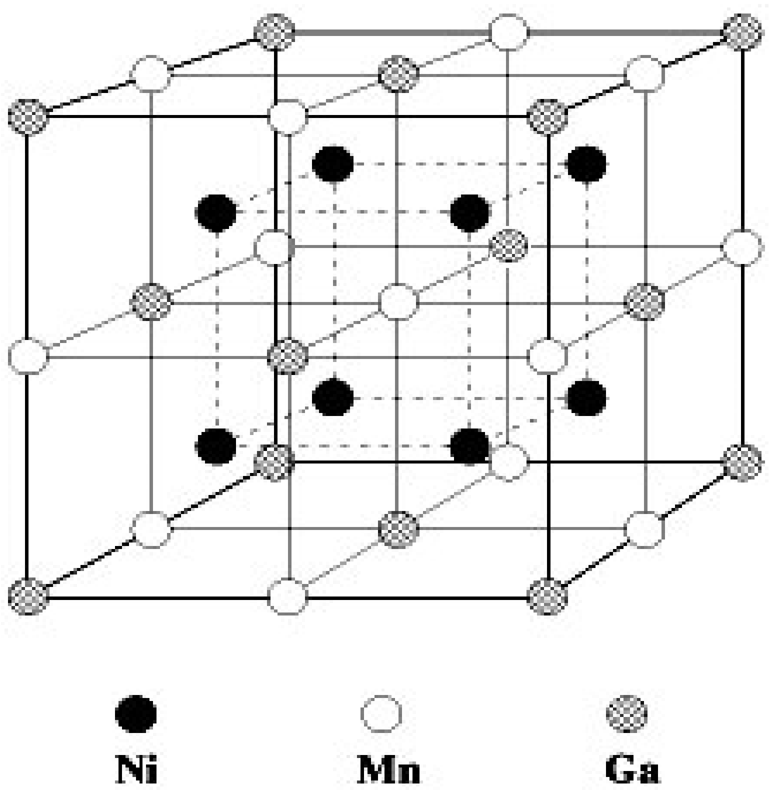

L21 structure: Four interpenetrating f.c.c. sublattices with :

✓Ni at (1/4,1/4,1/4) and (3/4,3/4,3/4)

✓Mn at (1/2,1/2,1/2),

✓Ga at (0,0,0).

➢Ferromagnetism due to RKKY indirect exchange interaction.

➢Heusler alloys are famous for localized large magnetic moments on Mn.

Crystal structure at room temperature

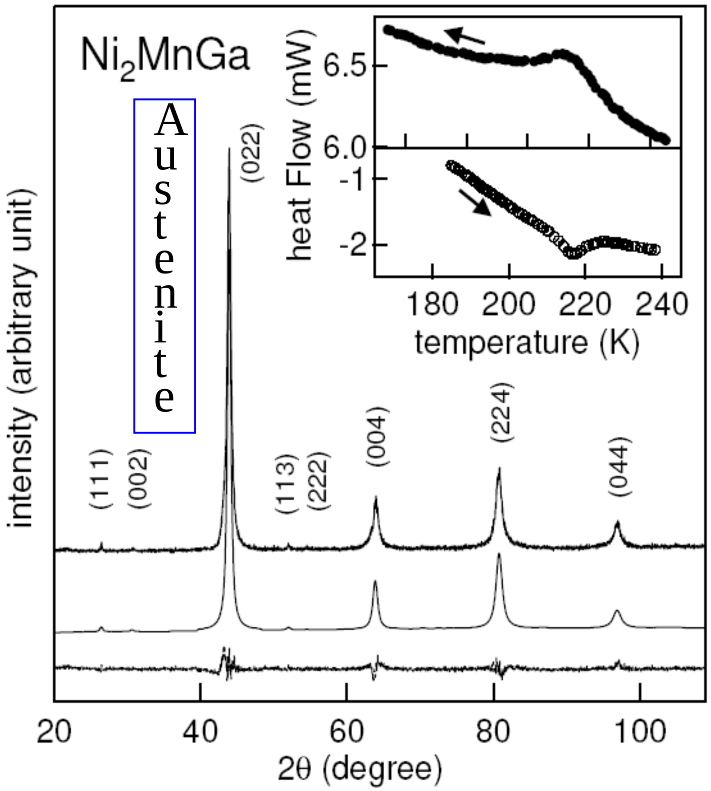

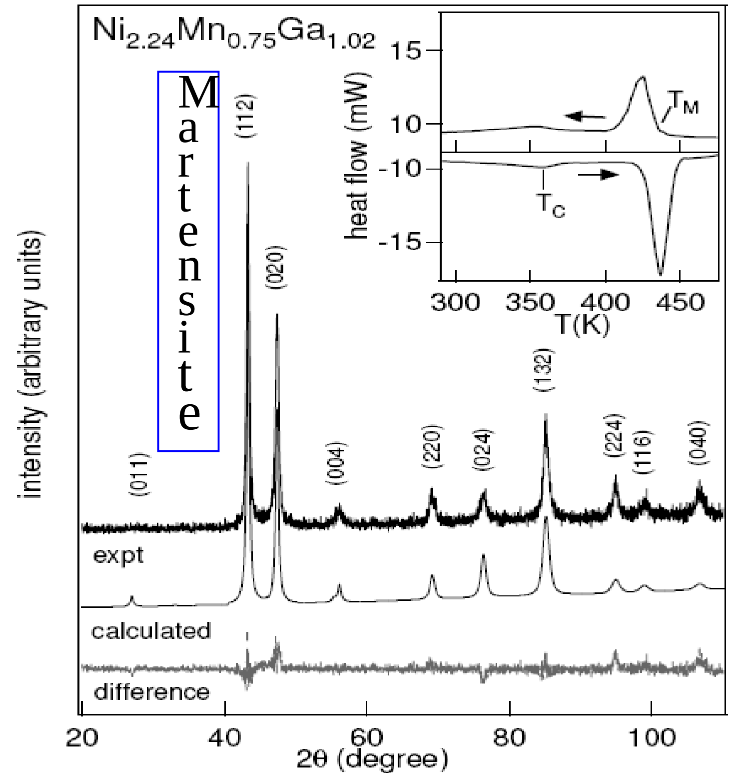

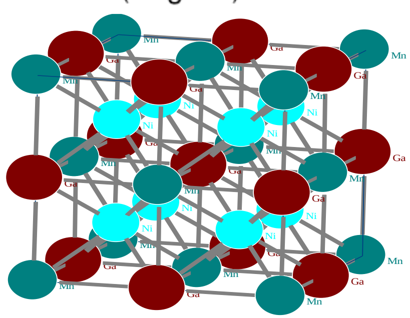

Cubic

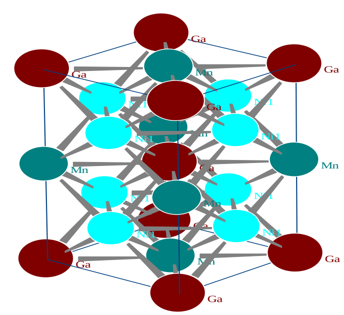

Tetragonal

Martensitic phase at room temperature.

DSC and ac-susceptibility of $Ni_{2+x}Mn_{1-x}Ga$

x	M_s (T_M)	M_f	A_s	A_f
0	205	189	216	234
0.24	434	408	423	447
0.3	537	523	553	582

DSC: [Rate 10 C/min]

Susceptibility: [26 Oe field, 33.33 Hz]

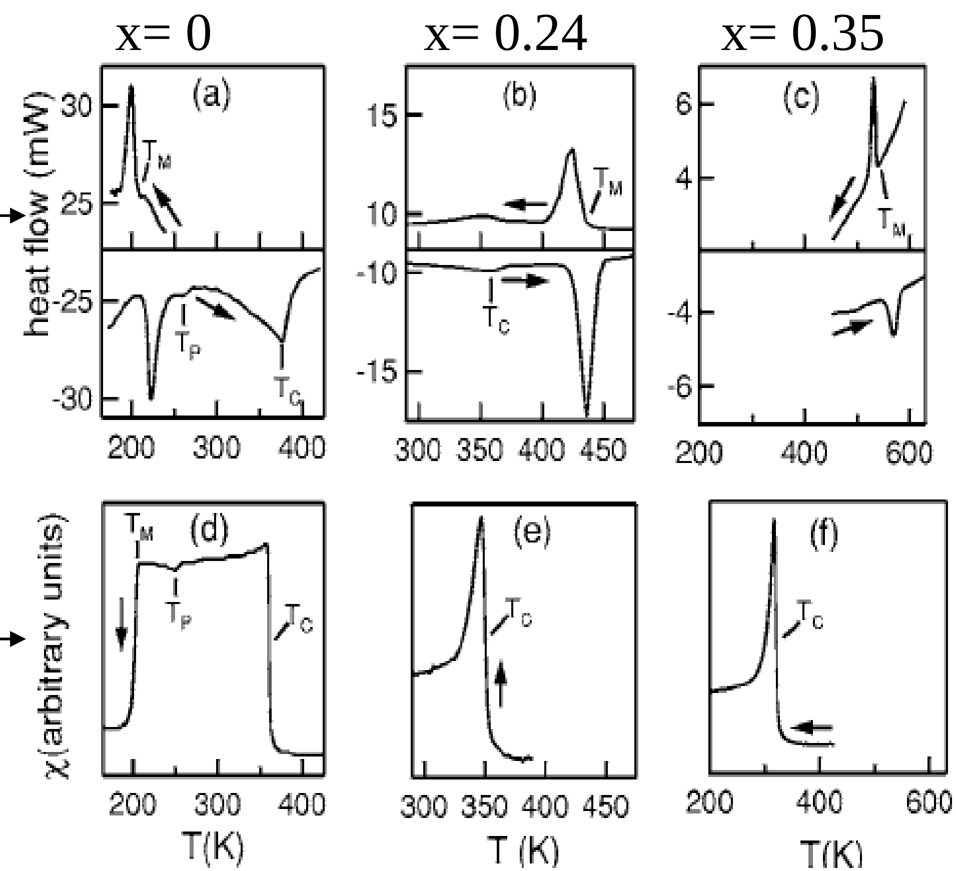

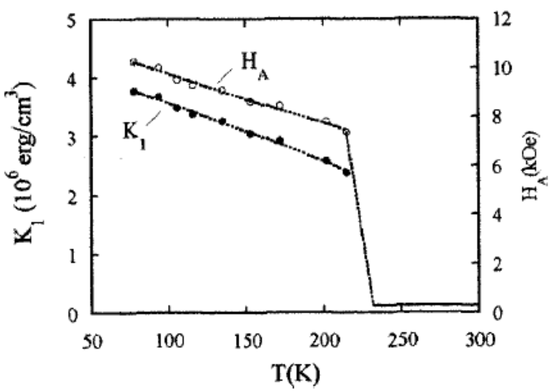

FIG. 5. Temperature behavior of the second order anisotropy constant (K_1) and of the internal anisotropy field (H_A) of polycrystalline Ni_2MnGa in the martensitic phase. The solid line indicates the upper limit for H_A in the austenitic phase. *Albertini et al, JAP, 89 5614, 2001*

Small width of hysteresis 14-38 K for x=0; highly thermoelastic (mobile interface, strain less).

Decrease of χ at T_M due to large magnetocrystalline anisotropy in martensitic phase. For x>0.2 TM>TC: change in χ shape.

Banik, Chakrabarti, Kumar, Mukhopadhyay, Awasthi, Ranjan, Schneider, Ahuja, and Barman, PRB, 74, 085110 (2006)

Ni-Mn-Ga is ferromagnetic, and exhibits magnetic SMA

SMA: Transformation from the martensite to austenite phase by temperature or stress.

FSMA: Entirely within the martensite phase, actuation by magnetic field, faster than conventional stress or temperature induced SMA.

10% Magnetic Field Induced Strain in Ni50Mn30Ga20 reported.

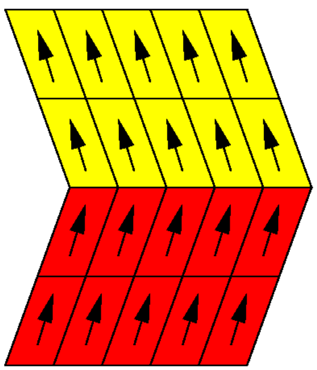

The magnetic moments without the external field

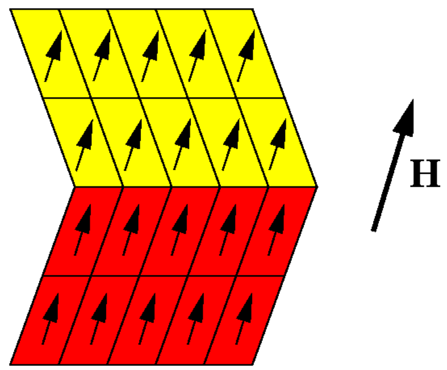

The rotation of the magnetic moments within the twins.

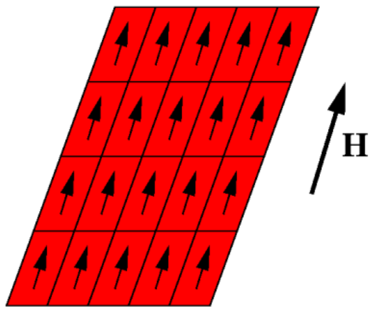

The redistribution of the twin variants.

Phase coexistence in Ni_2MnGa

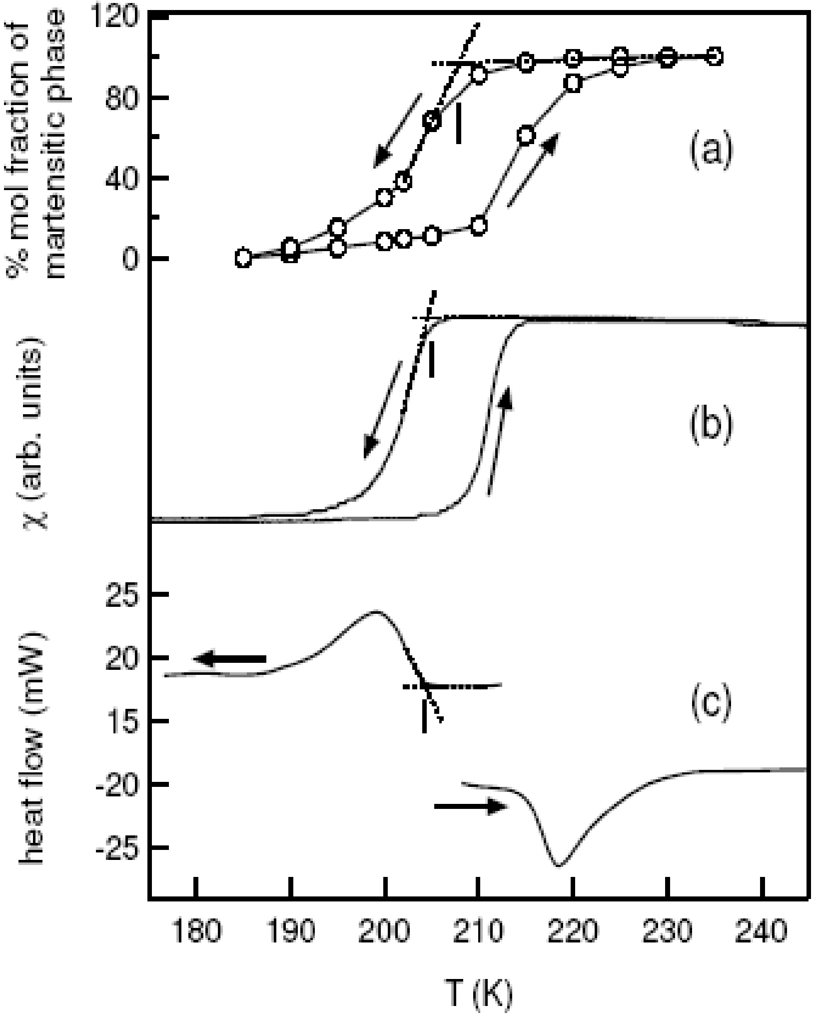

(a) Hysteresis curve showing mole fraction of the cubic phase determined from Rietveld analysis of the XRD patterns.

(b) Ac-susceptibity; Decrease at T_M due to large magnetocrystalline anisotropy in martensitic phase.

(c) Differential scanning calorimetry

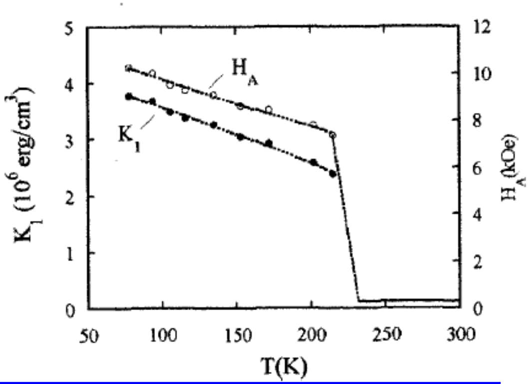

Nice agreement between structural, magnetic and thermal techniques. Small width of hysteresis 14-38 K; highly thermoelastic (mobile interface, strain less).

Resistivity and magnetoresistance

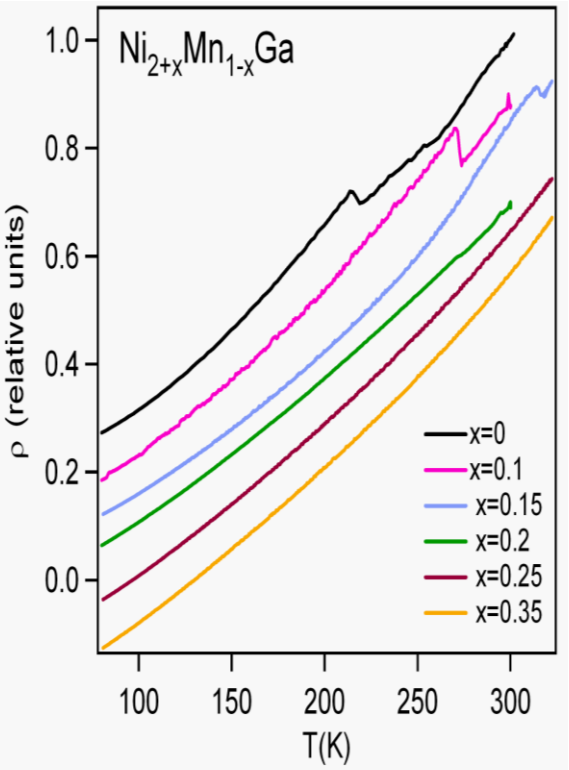

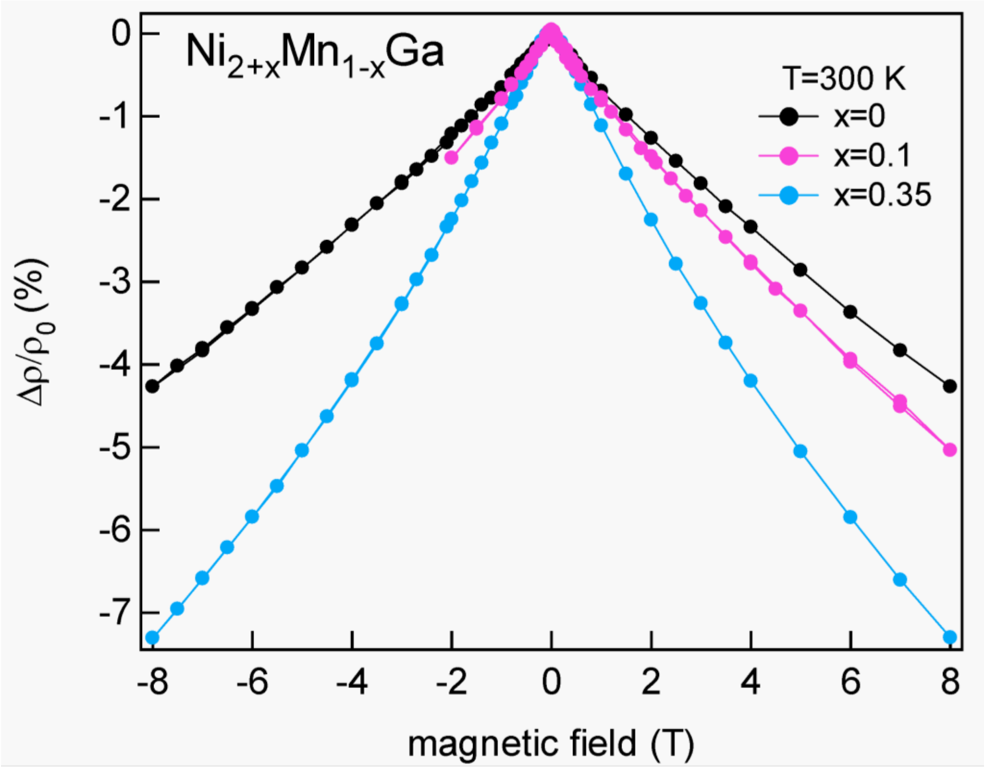

Metallic behaviour with a clear jump at T_M.

- Highest known magnetoresistance at room temperature for shape memory alloys. For x=0.35, MR is around 7.3% at 8T.
- Experimental MR behavior agrees with the theoretical calculation.

C. Biswas, R. Rawat, S.R. Barman, Appl. Phys. Lett., 86, 202508 (2005)

Smart actuator materials

Potential fields of applications

Actuator

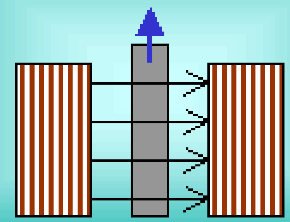

Couplers

- Fasteners
- Brakes and clamps
- Automatic assembly

Vibrators

- Shakers
- Sonar transducers
- Loudspeakers
- Drills
- Vibration damping

Fluidics

- Valves
- Pumps
- Injectors
- Ink-jets
- Drug delivery

Positioning devices

- Robots
- Manipulators
- Linear drives
- Switches

Sensors and generators

- Force/position sensors
- Vibration monitoring
- Joysticks
- Power generators

$Ni_{45}Co_5Mn_{40}Sn_{10}$.
The low temperature phase is nonmagnetic but the high temperature phase
is a strong magnet, almost as strong as iron at the same temperature."
The researchers immediately realized that such an alloy could act like
the phase-transitioning water in a power plant.
If you surround the alloy by a small coil and heat it through the phase transformation,
the suddenly changing magnetization induces a current in the coil," said James.
"In the process the alloy absorbs some latent heat. It turns heat directly into electricity."

Hysteresis and unusual magnetic properties in the singular Heusler alloy $Ni_{45}Co_5Mn_{40}Sn_{10}$
Vijay Srivastava, Xian Chen and Richard D. James
***Applied Physics Letters*, 97, 2010.**

A mi csoportunk hozzájárulása a
„Ferromágneses emlékező ötvözetek” témájához:
Együttműködve a Delhi Egyetemmel:

Appl. Phys. Lett. 97, 122505 (2010) Ni-Mn-Ga

J. Appl. Phys, 109, 083915 (2011) Ni-Mn-Al

1. Saurabh Kumar Srivastava, Vijay Kumar Srivastava, Lajos K. Varga, Vladimir V. Khovaylo, Ryousuke Kainuma, Makoto Nagasako & *Ratnamala Chatterjee*, “Systematic study of structural, transport, and magnetic properties of $Ni_{52+x}Mn_{26-x}Al_{22}$ (1 <x <5) melt-spun ribbons”, **J. Appl. Phys. 109**, 083915 **(2011)**
2. Saurabh Kumar Srivastava, Vijay Kumar Srivastava, Anupam Joshi, Pawel Kamasa, Lajos Károly Varga, V. V. Khovaylo & *Ratnamala Chatterjee*, “A low temperature anomaly observed in off-stoichiometric Ni–Mn–Ga system studied by higher harmonic ac-susceptibility measurements”, **Appl. Phys. Lett. 97**, 122505 **(2010)**

We have worked on the following aspects:

Single Crystal

- **Evidence of intermartensitic phase in single crystal Ni-Mn-Ga- magnetically & electrically verified**

- **Observation of three martensitic phases in Ni-Mn-Ga single crystal- in magnetic measurements**

- **Effect of twin boundaries on electrical properties**
- Crystal structure identification of different martensite phases by low temperature X-ray diffraction

Bulk Polycrystals

- **Series $Ni_{53+X}Mn_{25-X}Al_{22}$ (X=0,±1,±2) prepared and** detailed Structural property studies of the alloys prepared by different heat treatment

- Magnetic properties of the Aged Sample

- Magnetic and electrical properties of annealed samples followed by equilibrium cooled

XRD of NiMnGa single crystal

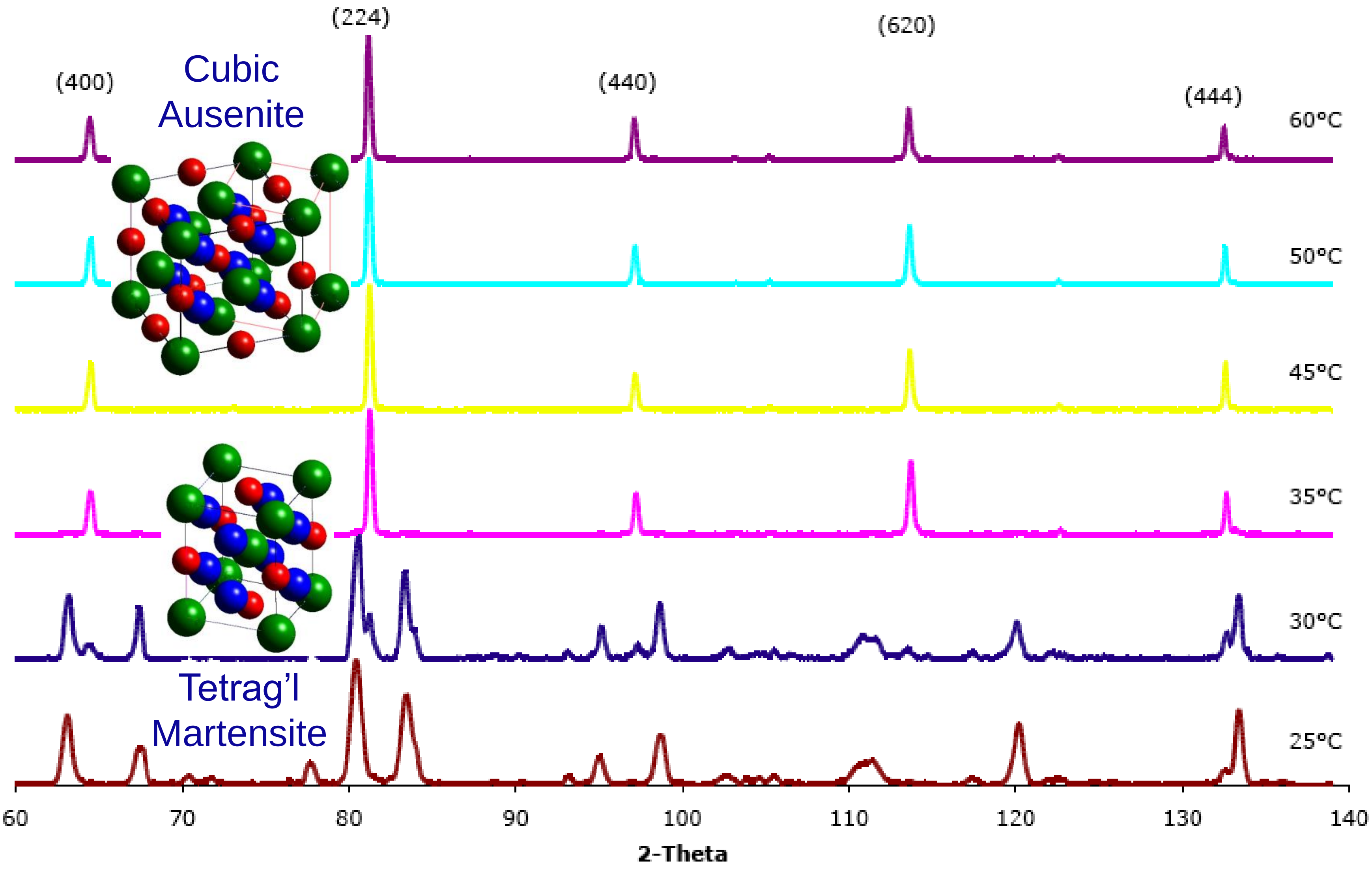

$Ni_{49}Mn_{29}Ga_{22}$

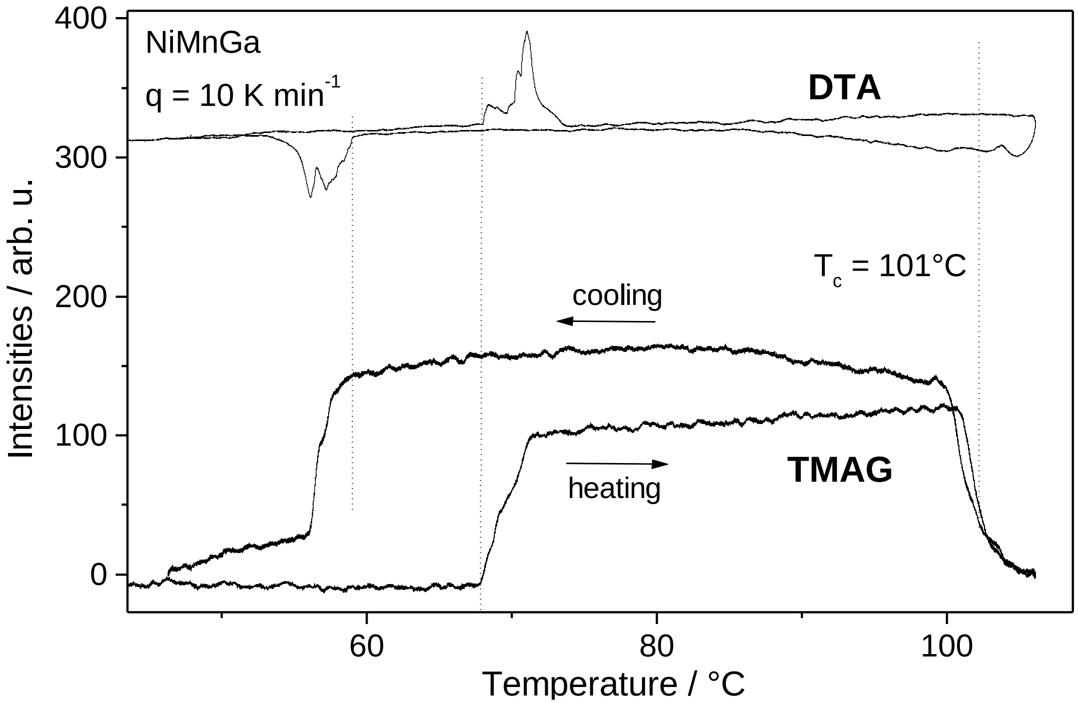

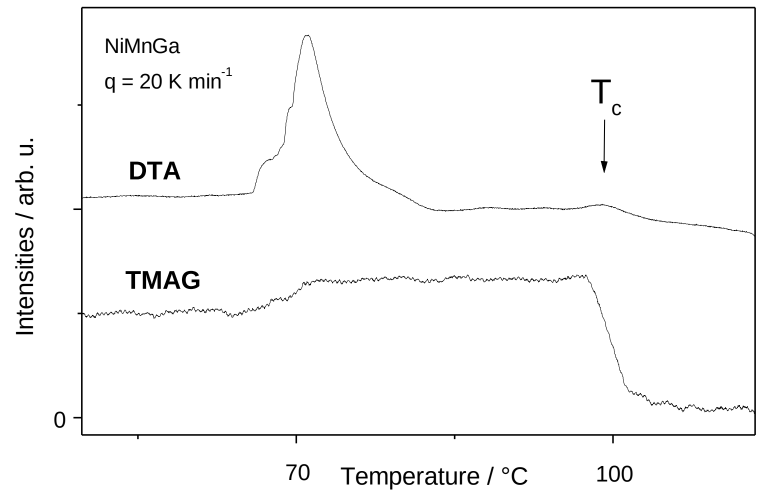

M-A and A-M transition with hysteresis of about 5 K

Curie transition is free from hysteresis and was recorded at around 100°C.

$Ni_{49}Mn_{29}Ga_{22}$

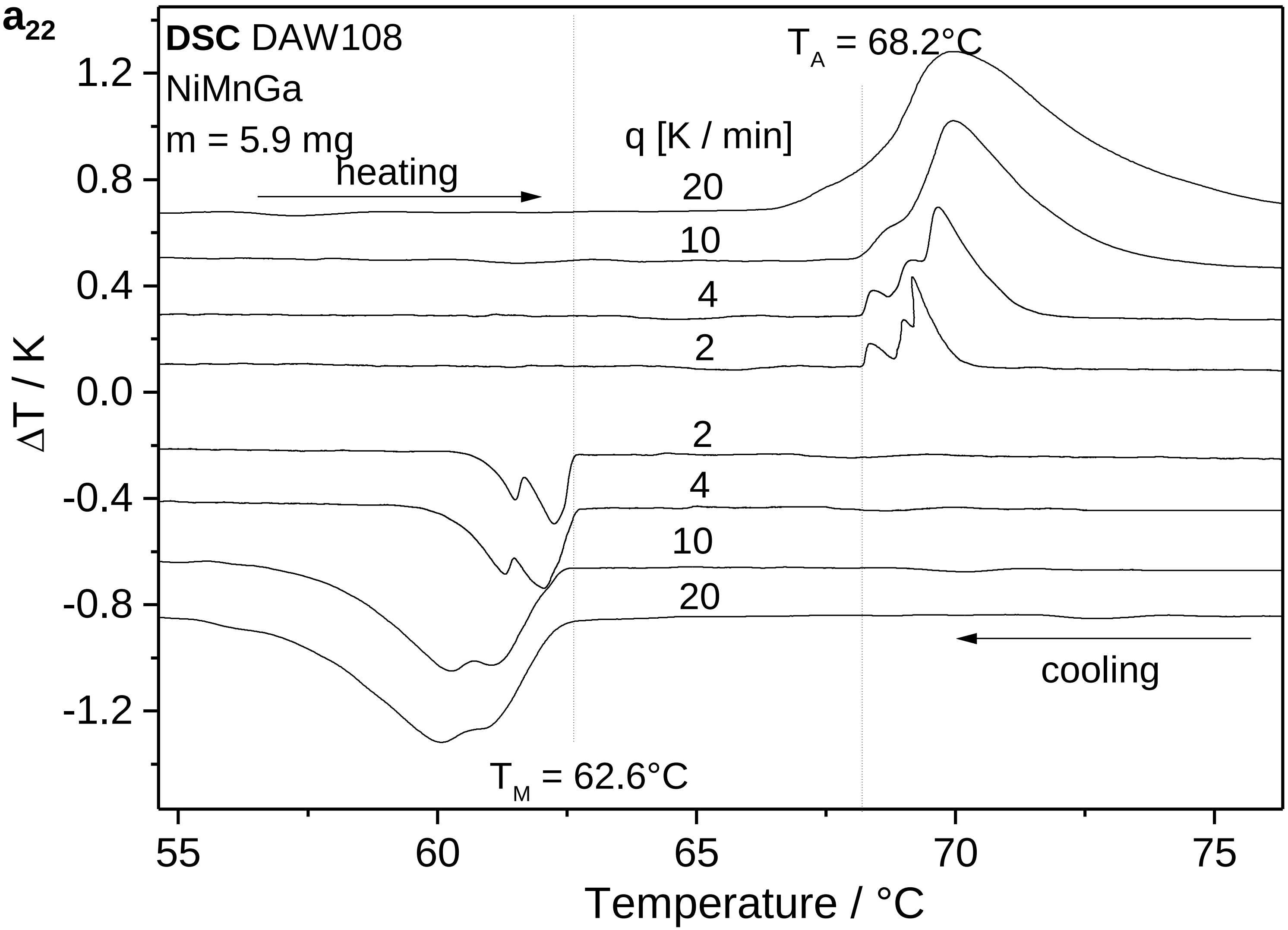

Phase transition temperatures for heating and cooling with rates between 20 and 2 $Kmin^{-1}$

$Ni_{49}Mn_{29}Ga_{22}$

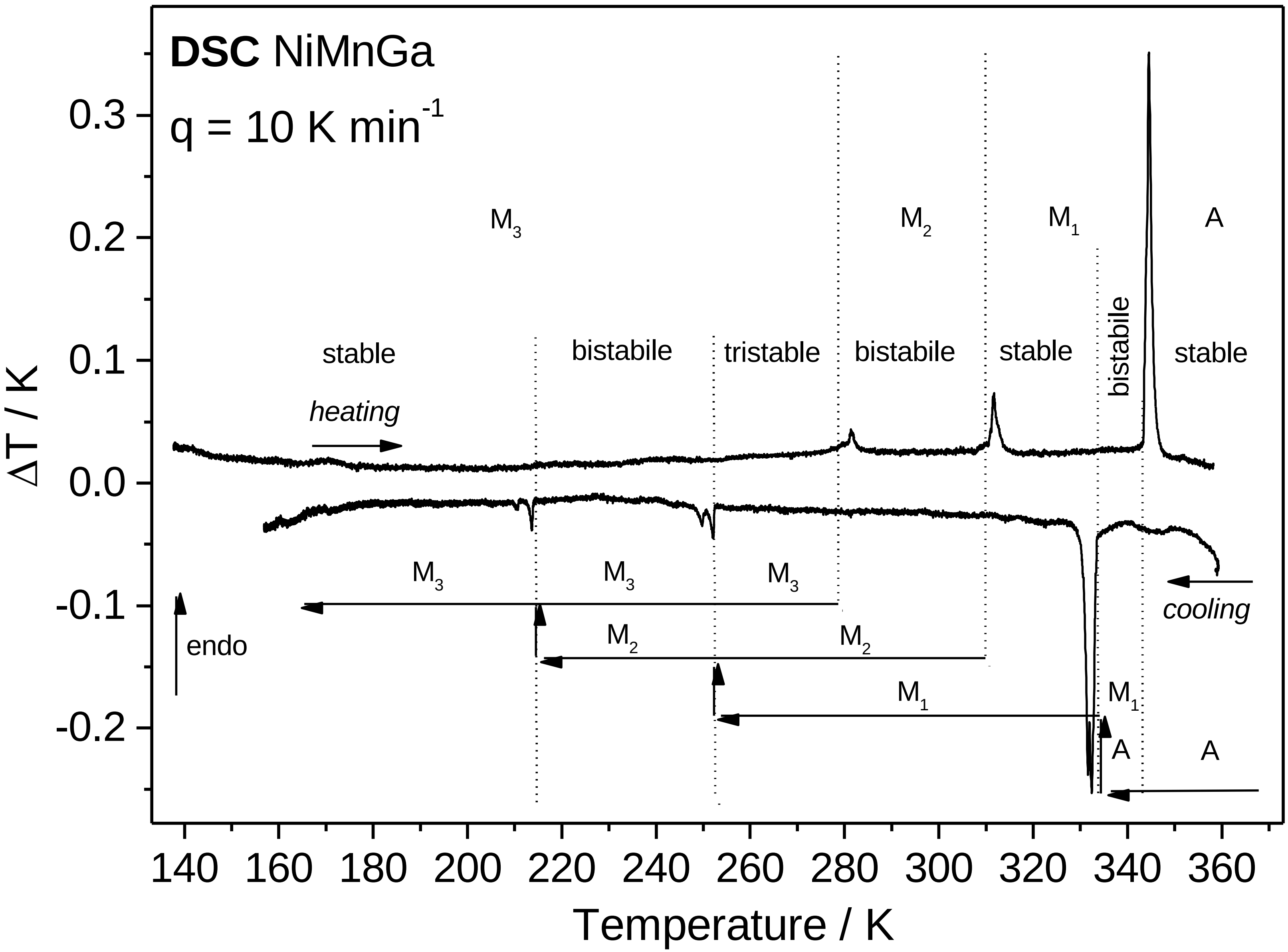

- Enthalpy of allotropic transformation is ~ 0.25 kJ/mol ~ same magnitude or even lower than the energy stored by cold working (Houska *et al,* Acta. Metall.**18**, 81, 1960)
- Assume a Molecular weight ~ 50g, density ~ 8g/cc $\Rightarrow$ 0.25 kJ/mol ~ 250J/50g = 5J/g

$$\Downarrow$$

martensite- austenite transformation

- On the other hand magnetocrystalline energy ~ 10^6 J/m^3 = 10^6 J/ 10^6cm^3 /8g/cm^3 = 1/8 J /g
- Zeeman energy : 1T*5000*80 A/m = 40*10^4J/m^3 = 40*10^4J/10^6cm^3/8g/cm^3 =5*10^{-2}J/g

Sample Preparation

Nickle Managnese&Aluminium of 99.99% purity

Pellets Of $Ni_{53-x}Mn_{25+x}Al_{22}$

Vacuum (2×10^{-5}) annealed, 1000^0C for 72 hours

Quenched in ice water ,Some samples are taken out for characterization

Some samples are aged in vacuum (2×10^{-5} Torr), 400^0C for 450 hours

χ vs. T of the Series

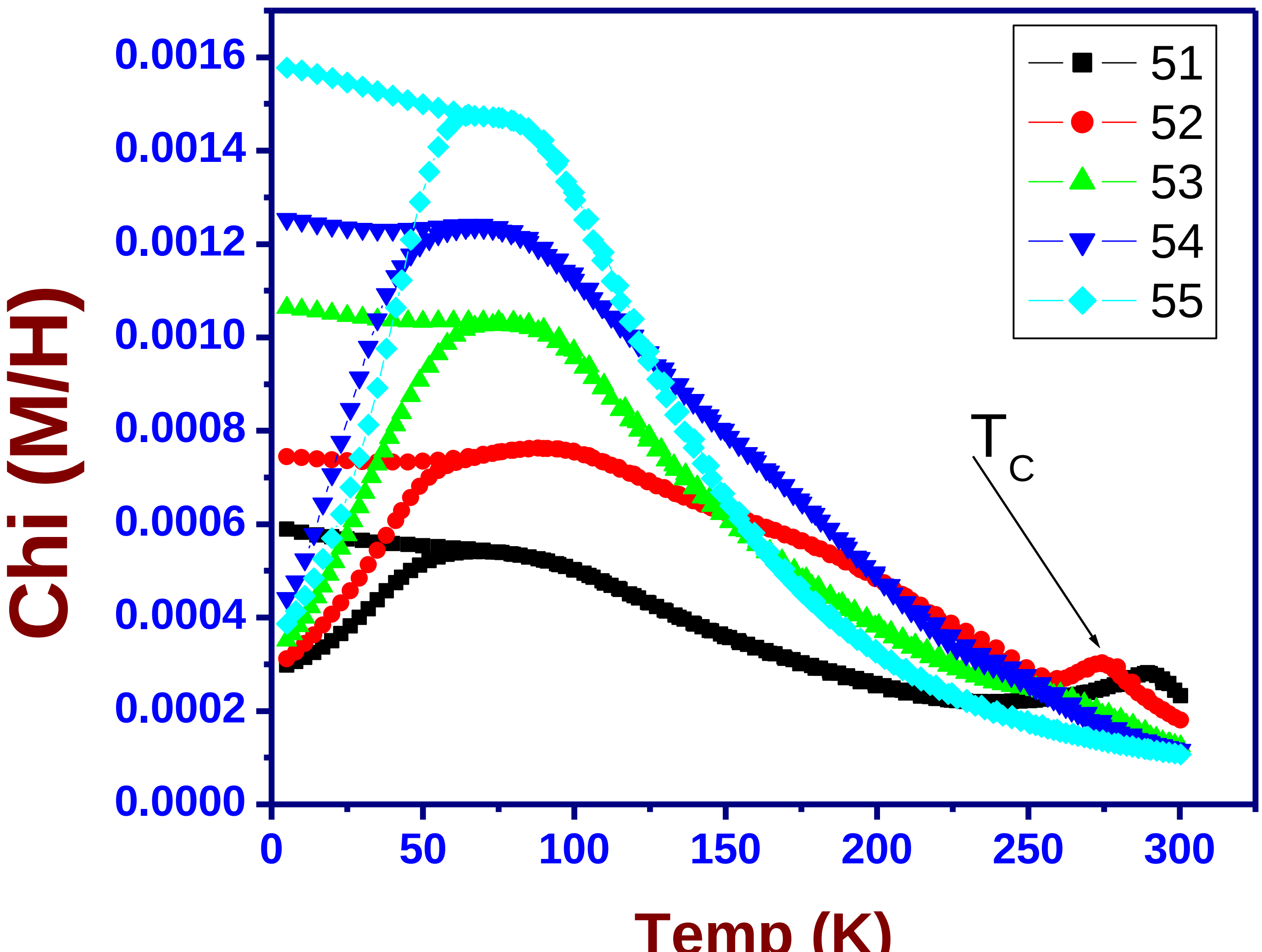

Electronic and structural transitions in $Ni_{52}Mn_{26}Al_{22}$ polycrystalline alloy

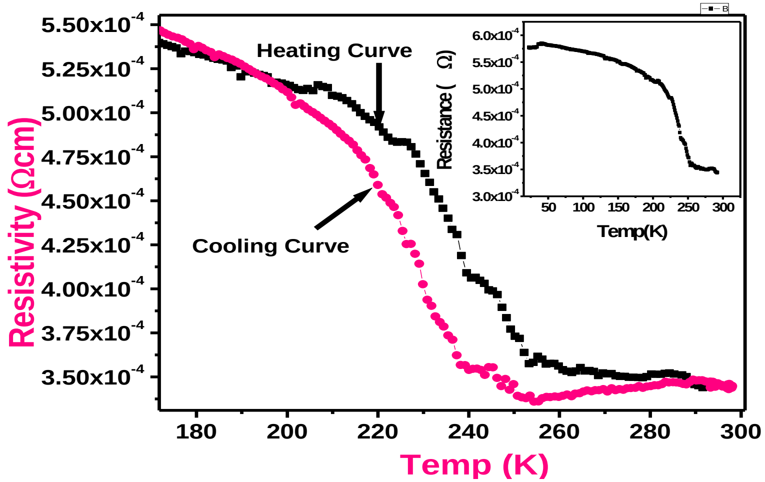

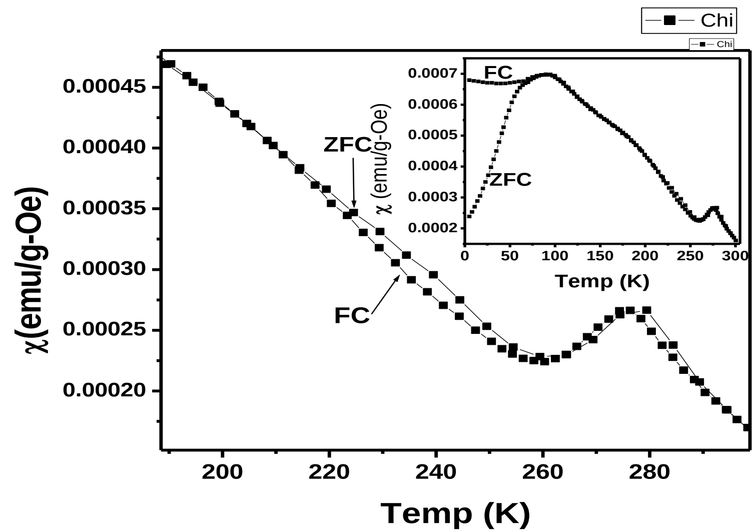

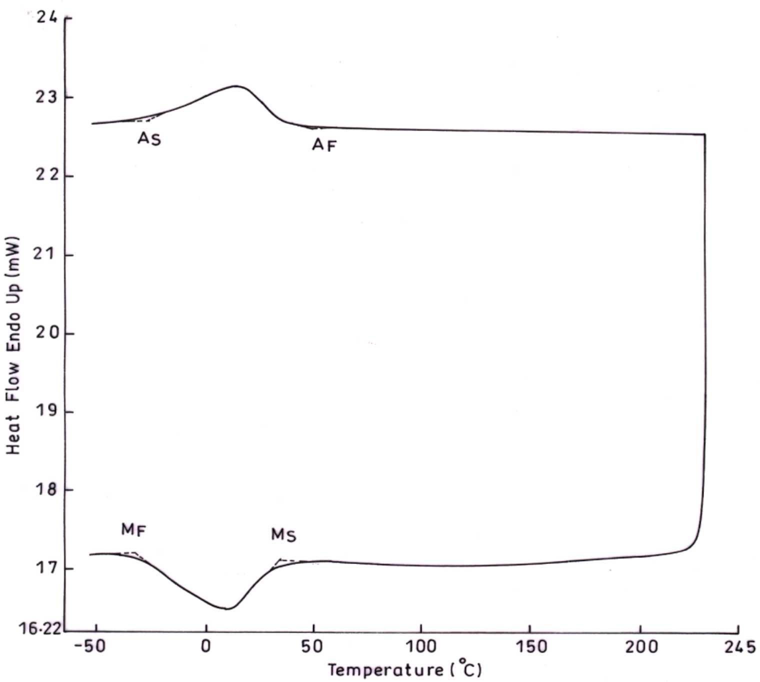

Property	A_s	A_f	M_s	M_f
Electrical	210	250	245	200
Magnetic	214	260	255	210
Structural	215	250	240	200

Comparison of the enthalpy and boundary friction energy obtained in the present case with the previous reports

Alloys	**ΔT (K)**	**T_0 (K)**	**ΔH J/mol**	**ΔS J/mol.K**	**F_r J/mol**
Cu29%Zn3%Al[a]	10	254	-416.2	-1.42	21.21
Cu14%Al2.5%Ni[b]	10	303	-515.0	-1.70	19
$Ni_{52}Mn_{23}Ga_{25}$[c]	6	311	-1617.2	-5.20	12.76
$Ni_{52}Mn_{26}Al_{22}$[d]	**35**	**247**	**-6748.46**	**-27.54**	**98**

[a] Y. Deng and G. S. Ansell, Acta Metall. Mater. **38,** 69 (1990)
[b] R. J. Salzbrenner and M. Cohen, Acta Matall. **27,** 739 (1979)
[c] Wong et al. Phys. Rev. B (2001)
[d] The present work